Calibration-Free Potentiometric Sensing With Solid-Contact Ion-Selective Electrodes

Celeste R. Rousseau and Philippe Bühlmann*

Department of Chemistry, University of Minnesota, 207 Pleasant St. SE, Minneapolis MN 55455, USA

*Corresponding author E-mail: buhlmann@umn.edu

Keywords: potentiometry, calibration-free, electrochemistry, solid contact, ion-selective electrodes

Abstract

In recent years, an important aspect of research into the improvement of ion-selective electrodes (ISEs) has been the development of solid-contact ISEs for calibration-free measurements, with the goal of sensors that can be implemented with ease for long-term, in situ analysis with very limited or no maintenance. This review discusses the definition of the term "calibration-free" in this context, and it gives suggestions as to what types of information should be reported if a claim of calibration-free usage is made. Relevant literature in this field is reviewed, with a focus on different mechanisms of ion-to-electron signal transduction. Different types of redox-active, capacitive, and mixed-mechanism transduction modes are discussed in view of the reproducibility and stability of the potential responses they provide.

1. Introduction

One of the greatest impediments to increasing the range of applications of many electrochemical sensors is the need for individual and frequent recalibration, which limits the speed of analysis and requires specialized equipment and knowledgeable personnel. Calibration-free potentiometric ion-selective electrodes (ISEs) in particular would allow for quick and easy use, which would simplify both medical and environmental analysis [1, 2]. Although this sounds appealing, it raises several questions: What does "calibration-free" mean? How should this term be defined, and what metrics can we use to measure the degree to which a system fits this description? As research continues to move forward, it will be important for those working in the field to agree on what the most important attributes of a sensor are if a study claims some level of "calibration-free" behavior. Moreover, those attributes will need to be reported consistently so as to allow the comparison of different approaches.

Before addressing this subject, it is helpful to consider what sorts of problems the availability of calibration-free electrochemical sensors would solve. Electrochemical sensors, and in particular ISEs, have been used routinely for both clinical and environmental analysis for many years [3-12]. The limitations of these sensors lie in the limited scope of applications in which they can be used reliably. ISEs are most often used for measurements in well-controlled laboratory settings such as in mainframe clinical analyzers. In the case of point-of-care measurements and continuous monitoring with wearable or implantable medical devices, the use of ISEs is hindered, although certainly not made impossible, by the need for (re)calibration. The applicability of such sensors in remote or resource-limited areas is further constrained by the need for maintenance. Similar limitations impede uninterrupted in-situ monitoring in the environment, which has great potential for studies of environmental processes and the early detection of contaminants in water resources. Coulometric readout for ISEs, which involves application of a constant potential between the ISE and reference electrode and integration of the observed current, has been proposed to provide a solution to the calibration problem [13]. However, while coulometry is inherently a calibration-free technique, it often requires an exact knowledge of the sample volume, although some methods have been shown to overcome this limitation. Moreover, the response time, which is typically on the order of several minutes, poses its own limitation [14].

Sensors to be used in a calibration-free manner need several important characteristics. For the most part, they require a miniaturized physical form, which is often achieved by the replacement of the inner filling solution of a traditional ISE with an alternative material capable of ion-to-electron signal transduction. This material, referred to often in the literature as a “solid contact” (SC) can be composed of a wide variety of materials. For more than 30 years, much

effort has been spent to develop solid-contact materials [5, 15-20] that facilitate ion-to-electron signal transduction and ensure stability and reliability of the potential response. The key differences between a traditional and a solid-contact ISE are displayed in Figure 1, along with an example of a standard ISE measurement setup with a representation of the phase boundary potentials in the system (general features of the theory of potentiometric measurements are discussed in Section 2 and Section 3.1). Features of an ideal solid-contact material have been discussed in several other reviews [21, 22], but no consensus has been reached to date as to what the term "calibration-free" exactly implies.

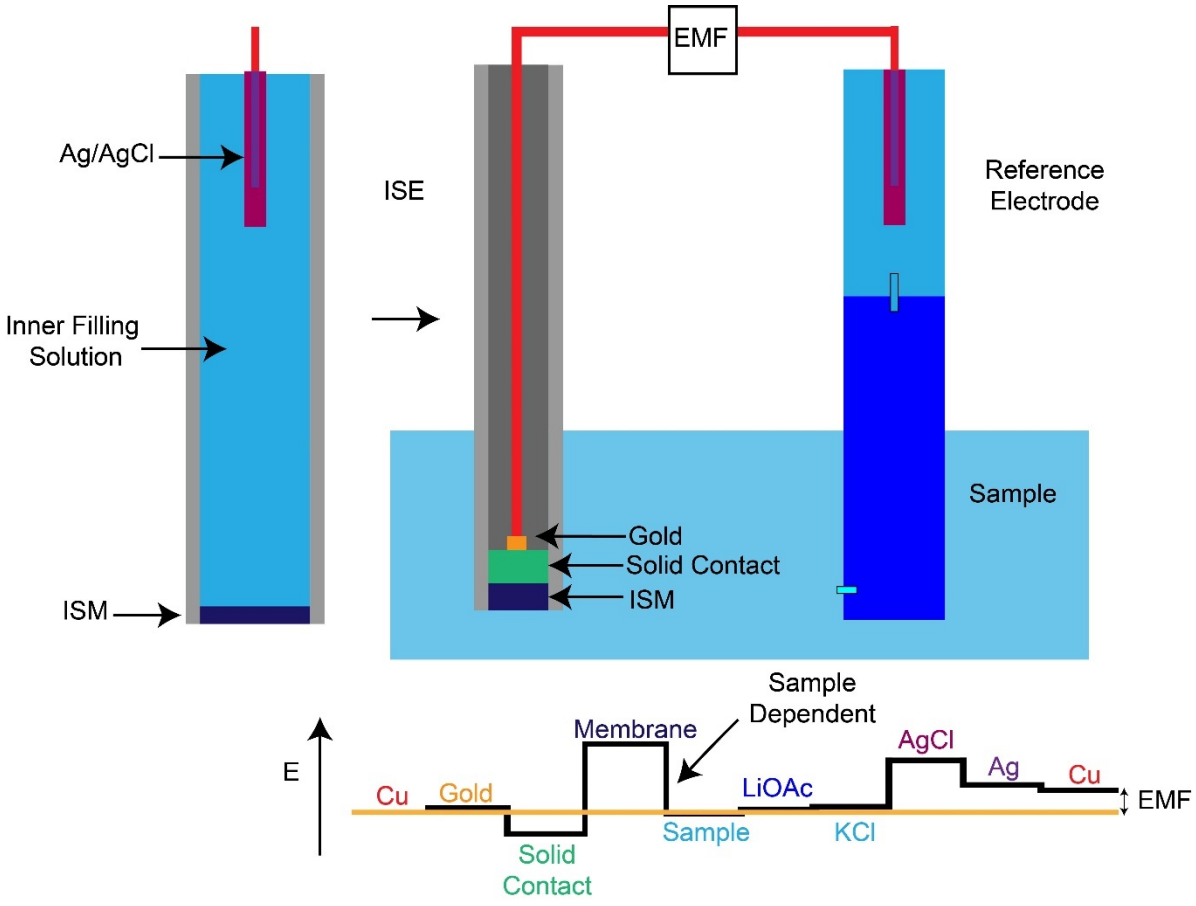

Figure 1. Comparison of a traditional inner filling solution ISE (left) with a typical solid-contact ISE (center, along with a representation of the phase boundary potentials arising at each interface in a potentiometric measurement using a solid-contact ISE and a conventional reference electrode (right). In an ideal currentless measurement, the measured EMF equals the sum of all phase boundary potentials.

2. Definitions of Calibration-Free Performance

2.1 Two Important Characteristics: E^0 Reproducibility and EMF Drift

The response of an ISE to the target ion is described by the Nernst equation:

$$E = E^0 + R\,T/(z_i\,F)\,\ln a_i \qquad (1)$$

where R, T, and F are the universal gas constant, the absolute temperature, and the Faraday constant, and z_i is the charge of the target ion, also referred to as the primary ion. E, the measured potential, is also referred to as the electromotive force (EMF). The E^0, also referred to as the standard potential, is the potential measured at a primary ion activity of 1 [10]. Actual measurements at such a high activity are usually not carried out, as such high concentrations can exceed the upper detection limit of the sensor and sometimes even the solubility of the analyte ion. Moreover, at such high ion concentrations it can be difficult to determine reliable activity coefficients and to correct accurately for the liquid junction potential at the interface of the reference electrode and the sample [23]. Consequently, the value of E^0 is usually extrapolated from the Nernstian response portion of the calibration curve.

As emphasized by Lindner and Gyurcsanyi [22], the reproducibility of E^0 is the single most important criterion that should be considered when deciding whether a system can be considered calibration-free. Even if calibration-free behavior is not a primary characteristic of a

sensor, reporting of the reproducibility of E^0 is a metric important for comparing the performance of different potentiometric sensing systems. For those studies in which the E^0 reproducibility is reported, this value has been typically computed for a batch of identically prepared electrodes that were all calibrated simultaneously. In such a case, the value of E^0 is determined as the average of the E^0 values from the calibration curves of each individual electrode, and reproducibility is reported as the standard deviation of this data set. It has been noted that, although a value of E^0 along with a standard deviation for a single batch of sensors is informative, more information may be gleaned through the batch-to-batch repeatability of E^0, as shown by the variability of E^0 for different batches of electrodes [24]. The slope of the calibration curve is also important, but if the sensors are operating correctly, the slope deviates only minimally from the theoretical Nernstian value (i.e., 2.303 $R\,T\,z^{-1}\,F^{-1}$ per tenfold increase in primary ion activity or, at T = 293 K, for a monovalent ion 58.2 mV/decade), and the standard deviation of the response slope as estimated from the experimental data should, therefore, be small. There is no consensus on the extent of acceptable deviations, but in our experience a deviation of up to 2 mV/decade is within the error of measurements when calibration curves are measured in routine experiments over a range of a few magnitudes of activity. Any larger deviation raises concerns about the EMF reproducibility, drift and, therefore, the accuracy of ion activity measurements.

Non-Nernstian responses and EMF drifts are often observed when the surface of the sensing membrane is not in equilibrium with the sample due to, e.g., ion fluxes that result from exposure of the sensor to a high concentration of interfering ions prior to measurements in primary ion solutions [25]. Alternative causes for apparently non-Nernstian response slopes may be the occurrence of multiple ion complexation equilibria in the sensing membrane [26, 27] and

non-linearity of the response curve in the activity range of interest at the lower or upper detection limit [8]. The latter can be quite easily overlooked when the level of curvature is small but readily affects the determined slope[28].

A simple but surprisingly often overlooked means to recognize minor curvature of a response curve are the residuals of the linear regression, that is, the distance between the measured EMF and the fitted regression line. If all residuals are positive at the upper and lower end of the calibration curve but negative in its mid-section (or vice versa), the calibration is curved. When the number of data points is not sufficient for residual analysis, simply connecting the first and last data point with a straight line and checking whether all remaining data points fall below or above this straight line can give a quick indication whether the calibration curve may be non-linear. The possible error encountered when fitting a set of calibration points that includes curvature is exemplified with Figure 2. For the example shown, despite a seemingly excellent correlation coefficient of 0.994, the curved calibration curve has a response slope 6 mV/decade smaller than theoretically expected. Any interpretation of the response slope should not be based on the value of this slope alone but also its error, as estimated from the experimental data.

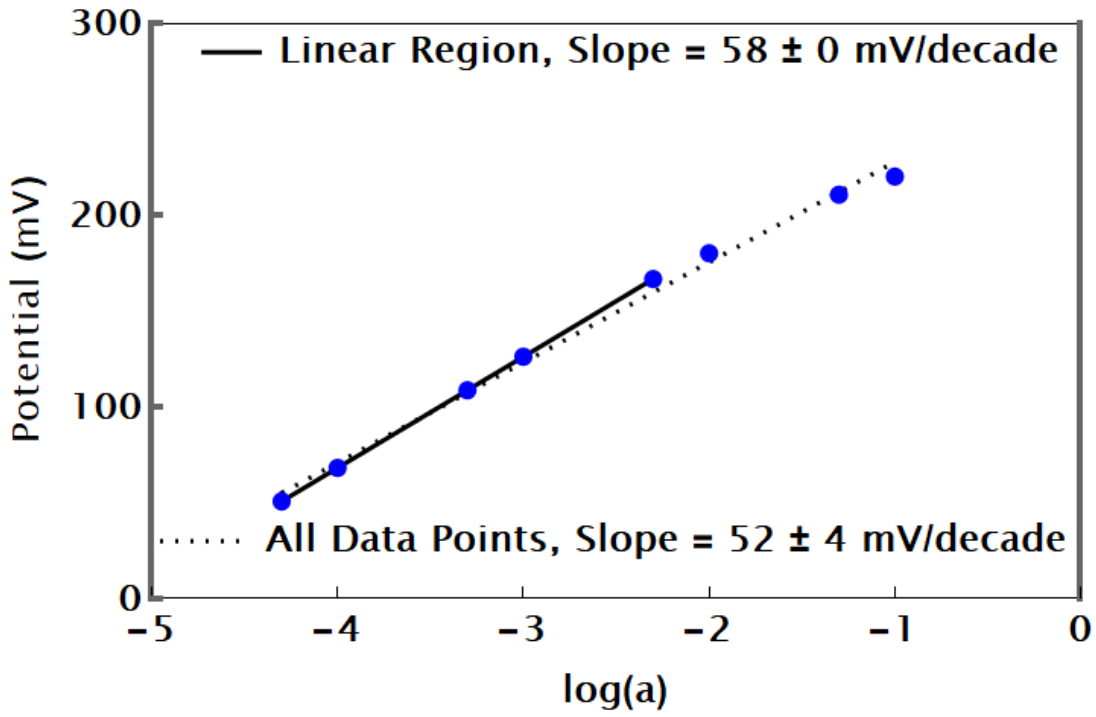

Figure 2. Example of curvature in an ISE calibration and the corresponding linear fits, with and without inclusion of the three data points with the highest primary ion activity. Error is reported as 95% confidence interval. For the data shown, the correlation coefficient is 0.994 when all data points are considered and 1.000 when only the five points at lowest activity are considered.

Many publications on ISEs report either a standard deviation of E^0 or a standard deviation of potentials measured at a particular experimental concentration. An interesting aspect of the problem of defining "calibration-free" performance and its relationship to slope reproducibility can be understood by looking at the difference between these two methods of reporting the potential reproducibility. This is illustrated in Figure 3. The *dashed* lines represent a set of three electrodes that have the same potential at, in this case, the arbitrarily chosen EMF of 250 mV at a concentration of 100 mM of the primary ion. This set of three electrodes has a slope standard

deviation of ± 1.0 mV and an E^0 standard deviation also of ± 1.0 mV. If the three calibration curves intersect at 10 mM while retaining the same standard deviation of their slopes, the E^0 standard deviation increases to ± 2.0 mV, as shown with the calibration curves represented as *solid* lines. Finally, the dotted lines in Figure 3 show what happens when the intersection of the three calibration curves occurs at 750 mM, while again the same standard deviation of slopes is retained. In this case, the E^0 standard deviation decreases to ± 0.125 mV. This demonstrates that, even in the case of small standard deviations of the response slope, the E^0 standard deviation can differ significantly from the standard deviation of the measured potential within the relevant concentration range of the intended primary ion. We conclude that the standard deviation for E^0, along with that of the response slope, should always be reported so as to provide metrics with which to compare work performed at different times and in different laboratories. In addition, reporting of the standard deviation of E in response to a representative primary ion activity is encouraged to accurately describe the sensor performance if the work is targeting a specific range of the primary ion concentrations, such as for measurements in clinical chemistry.

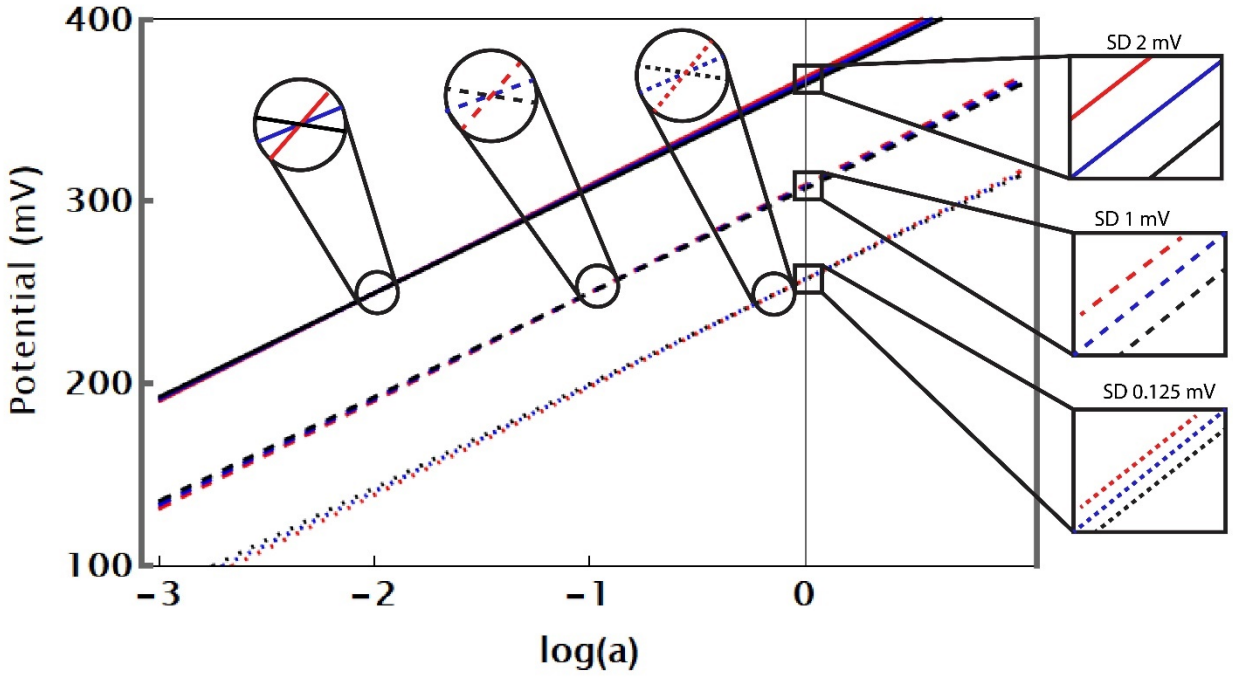

Figure 3. Comparison of three batches of three electrodes, with each batch having a slope standard deviation of ± 1.0 mV. The solid lines intersect at 10 mM, the dashed lines intersect at 100 mM, and the dotted lines intersect at 750 mM. The closer the intersection point is to 1.0 M, the smaller the calculated standard deviation of E^0. For each of the three batches, circular insets indicate the location of the intersection point and square insets highlight the standard deviation at 1 M.

Notably, if the acceptable error in ion activity is defined as a percentage of the true value, the corresponding acceptable deviation in the EMF response does not depend on the actual ion activity (see Figure 4). This is a direct consequence of the logarithmic dependence of the EMF on the ion activity, as shown in the following. The error in measurement (ΔE) given an acceptable percent error in reported activity, designated e_a , is obtained from

$$\Delta E = \frac{RT}{zF} \ln a - \frac{RT}{zF} \ln(a - e_a\, a) \tag{2}$$

and rearrangement gives

$$\Delta E = \frac{RT}{zF} \ln \frac{a}{a - e_a\, a} = \frac{RT}{zF} \ln \frac{a}{a(1 - e_a)} = \frac{RT}{zF} \ln \frac{1}{1 - e_a} \tag{3}$$

For example, if the error in ion activity must be <1.0%, then, for a monovalent target ion, the E^0 standard deviation must be less than 0.26 mV. If this acceptable error is as large as 5.0%, then the E^0 standard deviation can be 1.3 mV. The acceptable value of 0.7 mV quoted sometimes for sodium implies an acceptable deviation of 2.7%, which is based on the acceptable error in measurement of sodium concentrations as defined by U. S. Federal Regulations [21, 29]. This shows that the value of the acceptable percent deviation depends on the intended application and determines the acceptable error in the EMF measured by the ISE. It follows that whether a particular device can be called calibration-free is inherently defined by the application for which

it will be used. For a calibration-free device, if other sources of error can be ignored, the measurement error equals the error in E^0.

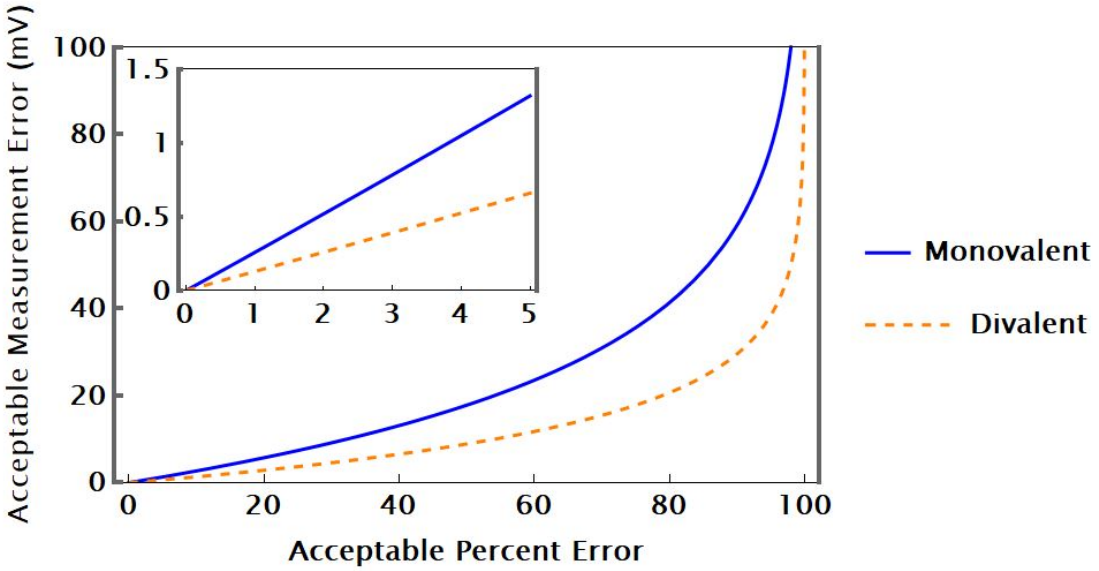

Figure 4. The acceptable error in a potential measurement for both monovalent (solid line) and divalent (dashed line) ions, as a function of the acceptable percent error in concentration from 0 to 100 percent error, and from 1 to 5 percent error (inset). The calculations used for this graph assume a temperature of 25 ºC.

Besides the reproducibility of the standard potential of several electrodes within a batch of electrodes or between different batches of electrodes, the drift of the EMF response is another important criterion for assessing for what applications a sensing system can be called calibration-free. It should be noted that for some longer-term applications a "calibration-free" sensor may not be required but a sensor that only needs to be calibrated once will suffice. In either case, any drift of the potential with time will eventually result in the loss of the validity of the calibration curve. This can be prevented by minimizing the drift of the electrode using suitable materials as

solid contacts. The magnitude of the EMF drift and the intended application will determine how long a sensor can be used before it must be calibrated again without unacceptable losses in accuracy. Figure 5 shows the time that can elapse between calibrations while maintaining reproducibility within an acceptable error in activity of 1.0%, 5.0%, or 10%. Results are shown as a function of the response drift, both for monovalent and divalent ions. Once the drift decreases below approximately 1.0 μV/h, the allowable time between calibrations increases greatly. For a drift of 1 μV/h, this leads to a time of 54 days between calibrations.

An important consideration when assessing long-term drift is drift of the half cell potential of the reference electrode. Any drift measurement is necessarily a combination of the total drift of the measuring and reference electrodes over the time period in question. This raises the possibility that drift of the reference electrode may obscure drift caused by the ISE. Therefore, in order to obtain accurate drift measurements, the drift of the reference electrode should be assessed and considered.

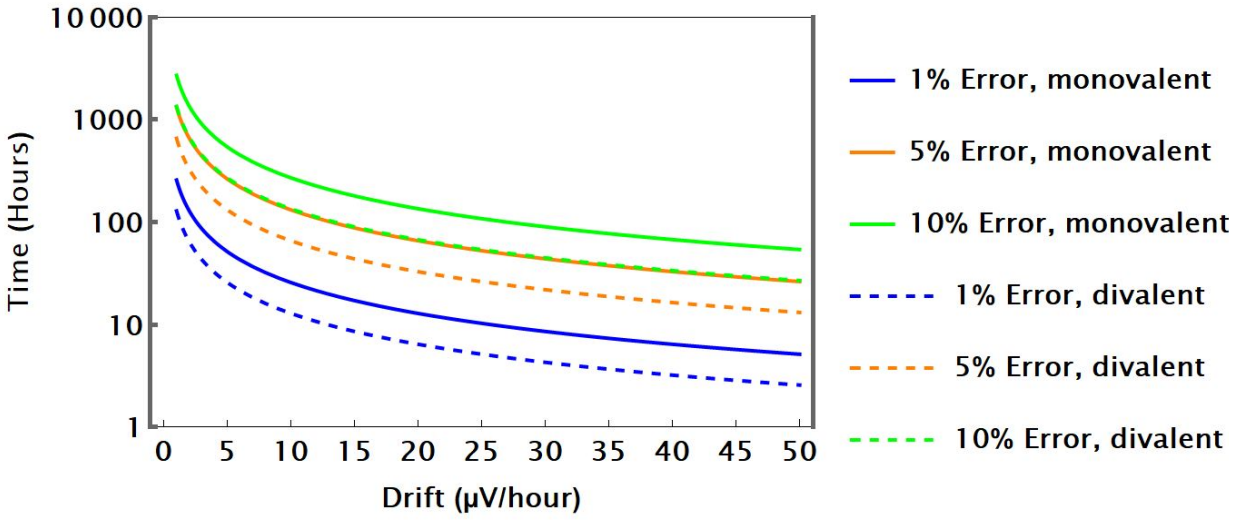

Figure 5. Maximum time between calibrations for 1.0%, 5.0%, and 10% error for signal drifts between 1 μV and 50 μV per hour, both for monovalent and divalent ions.

The above considerations lead to several key questions that can and should be asked in the context of any ISE that is intended to provide for calibration-free performance and, indeed, any system proposed to advance the field of solid-contact ISEs in a meaningful way, even if calibration-free performance is not required: What is the E^0 reproducibility, and how is this related to the reproducibility within the experimental concentration range? How does a single electrode's E^0 change over the course of time? How does the slope of the calibration curve change over time? What EMF drift do electrodes exhibit when stored in a solution of constant composition? And perhaps the most difficult question to answer, but a question whose answer provides significant insight: What are the processes that cause EMF drift and limit the reproducibility?

2.2 Causes of E^0 Variability

If calibration-free electrodes are to be realized, there are some practical recommendations to be considered. Firstly, it is important to realize that irreproducibility of E^0 can arise from variabilities in the phase boundary potentials at any of the interfaces in the electrochemical cell, not only at the phase boundary between the ion-selective membrane (ISM) and the electron conductor. It was pointed out recently that in particular the reproducibility of the phase boundary potential at the interface between the ISM and the sample solution should not be ignored [30]. This conclusion was based on experiments showing that the in-batch reproducibility of potentials was better for electrodes with a conducting polymer solid-contact layer in contact with an organic electrolyte solution (i.e., a tetrakis[pentafluorophenyl]borate solution in acetonitrile) than for measurements in aqueous primary ion solutions after deposition of an ISM onto the conducting polymer solid-contact layer.

It should be noted too that another source of irreproducibility may be the interface between the ISM and the SC. This could be a result of diffusive mixing of the ISM and solid contact over longer periods of time [31] or other slow processes that are not at equilibrium yet when the electrodes are being used. In studies of sensors designed to be calibration-free, investigations into the reproducibility of individual or smaller subsets of interfaces are desirable to clarify the extent of contributions from individual phase boundaries to the overall variability.

Moreover, while diffusion potentials within ISMs are rarely larger than a few millivolts [32], they do affect the measured E^0, e.g., after extended exposure of the ISM to solutions of interfering ions in selectivity measurements or water layer tests has resulted in extensive ion exchange with the sample. Therefore, efforts to assure that ISMs are free of interfering ions when E^0 values are determined are recommended. Advice that one should not forget the ISM when considering E^0 reproducibility is indeed well taken.

If an ISE membrane is not fully conditioned when a measurement is carried out, significant drift and E^0 variability can be expected. The conditioning time of solid-contact ISEs using various underlying conducting substrates has been studied using PEDOT(PSS) as the solid contact, showing that while the behavior of gold and glassy carbon was similar, platinum electrodes required significantly longer conditioning times [33]. It should also be noted that ISEs with thin membranes, and therefore shorter conditioning times, can result in faster display of degradation of the potentiometric response as a result of long-term processes [34], indicating that using sensors with short conditioning times decreases the time required to detect deterioration of solid-contact ISE. Of course, the definition of when a conditioning period ends depends on what the acceptable potential drift is for a given application. Sensors with a short conditioning time are advantageous in terms of ease and speed of implementation in applications where speed of

measurement with single use sensors is a primary concern, while a longer conditioning time is less of an impediment for applications that are longer-term. Additionally, even for those applications where the speed of analysis with a single-use sensor is critical, sensors that are calibration-free and stored and shipped in a manner that allows them to be used without lengthy conditioning fit this purpose, as has been demonstrated by the lowering of the conditioning time to a few minutes after storing sensors in a humid environment [35].

Variability in E^0 can also be caused by the underlying electron conductor, as the quality of the surface that makes contact with the solid-contact material can affect the observed response [24]. When gold is used as the material onto which the solid-contact material is deposited, a 3:1 volume mixture of sulfuric acid and 30% hydrogen peroxide, sometimes referred to as piranha solution, can be used to obtain very clean surfaces [36]. In research laboratories where individual electron conductors are used repeatedly to fabricate different devices, it may be worth considering the past exposure of these electron conductors to potential organic or inorganic contaminants to devise proper cleaning procedures to gain the highest E^0 reproducibility. Other considerations include the purity of all reagents being used, as well as procedures for the deposition of membrane and solid-contact materials from solution or dispersion, and whether these processes can be accomplished in a way that prevents unmixing of the components of the ISM or solid-contact material, resulting in inhomogeneities. It has been shown that membranes based on poly(vinyl chloride) (PVC) may exhibit an asymmetrical distribution of plasticizer between the upper and lower sides of the membrane [37], and small angle neutron scattering has shown the presence of crystalline PVC regions within plasticized membranes as well as water droplets [38].

The value and reproducibility of E^0 evidently depends on the level of doping of conducting polymers used as ion-to-electron signal transducer. Another factor, i.e., the effect of structural variabilities on E^0, is less well understood. However, the conductivity of poly(3-octylthiophene) (POT) can be affected by whether a film of this material is produced using spin-coating or drop-casting, which is the result of differences in the fraction of the polymer that is highly ordered [39]. In addition, the deposition technique used to prepare a conducting polymer film can affect the hydrophilicity of the resulting film. For poly(3,4-ethylenedioxythiophene) (PEDOT), e.g., it has been shown that electropolymerization results in a more hydrophobic layer [40]. Effects of such structural variation on E^0 would hardly be surprising.

Of particular importance to EMF drift is preventing the formation of a water layer between the solid-contact material and the underlying electrode, as pooling of water at this interface is detrimental to sensor performance [41, 42]. If such a water layer does form, ISMs not only delaminate readily [43] but the sensors also no longer function as true "solid-contact" ISEs. Instead, they have a very small aqueous inner solution, making the phase boundary potential at the interface of the ISM and this thin water film very sensitive to changes in the ionic content of that water film. Interestingly, the smaller the volume of this water layer, the faster its ionic content can change as a result of transmembrane ion fluxes, and, therefore, the faster the phase boundary potential at the interface of the sensing membrane and the water layer can change. This includes sensitivity to carbon dioxide, which readily diffuses through many ISM materials and upon dissolution in the water layer changes its pH. Indeed, sensitivity to CO_2 can be an indication of water layer formation [44], as similarly observed already in 1985 in the context of chemically modified field-effect transistors [45].

In order to prevent the formation of water layers, much effort has been focused on the development of solid contacts with high hydrophobicity, which is often assessed using the water contact angle of the solid-contact material. Larger contact angles indicate that the material is more hydrophobic (see Figure 6) [30, 46]. Use of an ion-selective membrane material that is more hydrophobic than, for example, the often used PVC plasticized with bis(2-ethyl hexyl) sebacate (DOS), can also slow down the formation of a water layer, as shown, e.g., for poly(methyl methacrylate)–*co*–poly(dodecyl methacrylate) ISMs [47].

It should also be noted that the type of transducing layer used can influence the rate of leaching of ionic sites or ionophore from the ISM. This was shown for sensors comprising carbon black, resulting in reduced loss into the sample of tetraphenylborate, which has a much lower hydrophobicity than substituted tetraphenylborate derivatives more commonly used in ISEs [48]. While the authors of that work did not speculate on the cause of this effect, it appears likely that it is related to adsorption of tetraphenylborate and ionophore onto the high surface area carbon, reducing the concentration of dissolved dopants in the ISM.

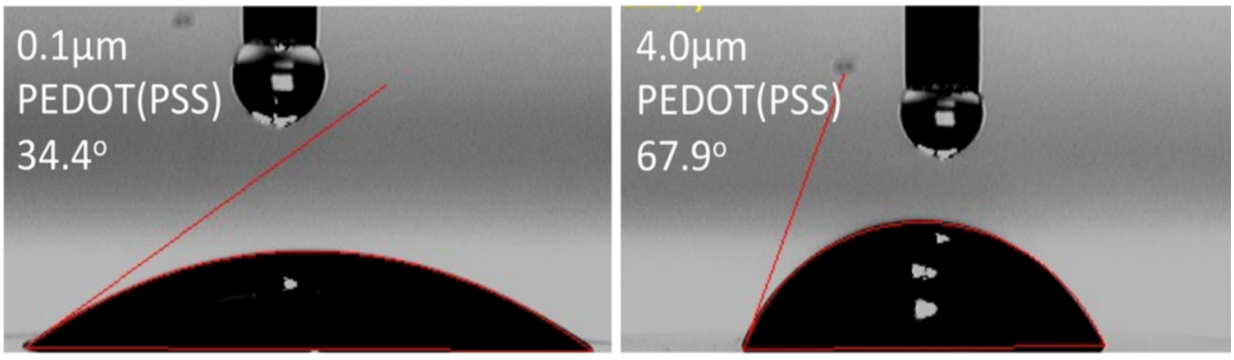

Figure 6. Example of a water contact angle on electrochemically synthesized PEDOT doped with poly(styrene sulfonate) (PSS), a common solid-contact material for ISEs. Thicker layers

of conducting polymer result in a larger contact angle, a result of changes in the extent of PEDOT oxidation with film thickness. Adapted with permission from reference 46.

Sensitivity to molecular oxygen, O_2, can indicate an insufficient redox capacity or insufficient chemical stability of the solid-contact material. To that end, many investigators bubble alternately pure oxygen and pure nitrogen through a sample into which the tested ISE is inserted and simultaneously monitor the EMF [20]. A slight sensitivity to pure oxygen in such an experiment may be considered acceptable, as the high concentrations of oxygen that affect the measured potential are unrealistically high for all but very few real-life measurement situations. Moreover, many real-life samples are in equilibrium with atmospheric oxygen, whose concentration varies only in a narrow range. However, a small, short-term sensitivity to oxygen is often indication of an irreversible chemical reaction of the solid-contact material with oxygen and, therefore, can be a harbinger of long-term drift.

Similarly, the light sensitivity of solid-contact ISEs is often tested. While one of the early and most investigated transducers, POT, is a light sensitive conducting polymer, smaller light sensitivities have been observed for polypyrrole (PPy) and (PEDOT) [49].

Especially if the material providing for the ion-to-electron signal transduction is directly mixed into the ISM as opposed to forming a separate layer, the redox sensitivity of the sensor should be assessed. In many research laboratories this is accomplished using sample solutions comprising varying ratios of the ferricyanide/ferrocyanide redox couple [16]. If the measured potential changes with this ratio, the sensor is probably sensitive to redox interferents in solution and is, therefore, not suitable for in situ measurements. Pitfalls are possible though, as an anion-

selective ISE may respond to the ferricyanide and ferrocyanide anions directly rather than the redox potential determined by these two species, and a cation selective ISE may respond to the cations of the ferricyanide and ferrocyanide salts needed to prepare the sample solutions. In either case, addition of the ferricyanide/ferrocyanide into relatively concentrated solutions of the primary ion of the investigated ISE substantially reduces the likelihood of such problems.

Another issue of note that deems mentioning is that of biofouling. If ISEs are to be successfully implemented in long-term, in-situ applications, where calibration-free electrodes would be especially effective, they must resist absorption and adsorption of biomolecules and other contaminants that can affect and degrade the response over time. This includes earlier work with NO releasing ISE membranes and polymeric materials [50, 51]. More recent methods to address this problem include polydopamine coatings [52], silicone rubber coatings [53], fluorous-phase membranes [54], 6-chloroindole release [55], and silver nanoparticles [56]. Truly calibration-free electrodes must possess high reproducibility, low drift, and resistance to (bio)fouling.

Table 1 summarizes our recommendations for analyzing and reporting the performance characteristics of solid-contact ISEs, both in general terms as well as in specific consideration of calibration-free uses. Note that a few of these recommendations may appear obvious but are included in this table anyway, on one hand to make the list comprehensive but also because there is a not insignificant body of published work that indeed lacks such information.

Table 1: Recommendations for Analyzing and Reporting Performance Characteristics of Solid-Contact ISEs and Reference Electrodes (REs)

Performance Characteristic	Recommendation(s)
Use of term "calibration-free"	• Define conditions under which calibration-free measurements are envisioned; this may include expected accuracy and period between calibrations (if any) or whether a one-time calibration is required.
Important ISE characteristics	• Report E^0, drift, selectivity, response slope, capacitance, and limit of detection, all along with standard deviations or estimated error.
ISE response slope	• Response slopes should not be used as single evidence for sensor durability after long periods of measurements or storage, as they may still be adequate even when selectivity losses already happened. • Check carefully for non-linearity at the upper and lower end of the linear response range, as this can result in large E^0 deviations even when correlation coefficients are very close to 1.00.
ISEs: Report E^0, or E at a selected target ion activity?	• Always report E^0 reproducibility; this enables comparison of work performed in different laboratories. • Report E within relevant range of primary ion concentrations (with the measured concentration reported) if a specific application is targeted, such as measurements in body fluids. • The standard deviation of the response slope should be considered when comparing differences between the standard deviation of E^0 and that of E.
E^0 reproducibility (ISEs and REs)	• Specify whether reported standard deviations represent one or several batches of sensors. • Reporting of batch-to-batch E^0 reproducibility is encouraged. • *For devices comprising redox buffer:* If possible, vary the ratio of reduced and oxidized components to assess its expected effect on E^0. This can help identify secondary effects, such as when a redox-active SAM fails to function as redox buffer but inhibits water layer formation.
EMF drift (ISEs and REs)	• Control the temperature if low EMF drifts are expected. • Test stability of the potentiometer (e.g., by short-circuiting a sensor channel with a reference channel using a resistor and measuring EMF over an extended period of time). • Test effect of oxygen and carbon dioxide (or alternative basic or acidic volatile species). • Test stability of ISE and reference half-cell independently (e.g., by measuring versus a AgCl-coated silver wire in a KCl solution). • Avoid qualitative statements such as "stable E^0 for several months". • The most common characteristic of long-term drift is $\Delta E/\Delta t$ from a linear regression of the EMF vs time curve.

Long-term measurements (ISEs and REs)	• Clearly specify electrode exposure during measurement (e.g., "continuous measurement in unstirred 1.0 mM NaCl solution for 10 days" or "stored in air in between measurements"). • Perform water layer test at end of long-term measurements to assess whether water layer formed during extended sample exposure.
Redox sensitivity (ISEs and REs)	• Assessed using solutions of redox-active ions; to avoid pitfalls, measurements with ISEs are best performed with high concentration background of primary ions.
Control experiments (ISEs and REs)	• The performance of devices with new types of signal transduction layers should include control experiments with devices of established design (ideally measured in parallel). • In the case of signal transduction layers comprising multiple components, control experiments should assess performance of devices with transduction layers comprising only subsets of those components.
RE characteristics	• Report E^0, drift, resistance, and capacitance, in all cases along with standard deviations or estimated error. • Describe effect of ionic composition of samples on E^0, in view of comparison with other work in particular for Na^+, K^+, H^+, Cl^-, HCO_3^-, and NO_3^-.
Potentiometer characteristics	• Many publications mention the type and manufacturer of the potentiometer used; also helpful to the reader is the potentiometer's input impedance, which along with the total resistance of the electrochemical cell determines cell current.
E^0 and phase boundary potentials	• All phase boundary potentials contribute to E^0; variability of the sample/ISM and ISM/transducer interfaces should not be ignored. • Experiments testing reproducibility of contributions from individual interfaces are encouraged.

3. Ion-to-Electron Signal Transduction

3.1 Categories of Solid Contacts Based on the Transduction Mechanisms

The key challenge to resolve in the design of calibration-free, solid-contact ISEs is the control of the potential at the interfaces between all contacting phases. Although all interfaces are important, the one to which the most attention has been given is that between the sensing membrane and the underlying electron-conducting substrate. In a traditional ISE, the sensing membrane is contacted on the backside by a solution, which is in contact with a AgCl-coated Ag

wire. Comparison with this system can be useful to assess the performance of newly proposed solid contact materials, although it should be kept in mind that rigorous studies in view of E^0 reproducibility have not been carried out with traditional aqueous inner contact electrodes. As outlined in previous review papers focusing on general characteristics of solid-contact ISEs, there are two broad categories of transducers that used to replace the traditional system, using different mechanisms, each of which has certain advantages [21, 22, 57, 58].

The first is analogous to the traditional Ag/AgCl inner reference element, an electrode of the second kind, where the solid contact possesses redox activity, providing for exchange of electrons between the electron conductor and a solid-contact material added to the interface of the ISM and the electron conductor. These redox-active solid-contact materials also exchange ions with the sensing membrane, providing a thermodynamically well-defined phase boundary potential.

The second possible mechanism involves placement of a purely electronic conductor with an extremely large surface area on top of the electrical contact. In the absence of a redox-active species, the interface of the ISM and such a high surface area conductor is polarizable, the large surface area providing it with a double layer capacitance that is much larger than for a coated-wire electrode or a flat conductor coated directly with an ISM. Using the relationship for voltage across a capacitor, $\Delta E=Q/C$, where Q is the charge and C is the capacitance, one can calculate the resulting interfacial potential. Accordingly, the larger the capacitance, the smaller the interfacial potential that develops for the same charge accumulated. Because current is equivalent to charge per unit time, this also means that, in the presence of small currents, the interfacial potential will change more slowly over time, the larger the interfacial area and, therefore, the double layer capacitance is.

Potentiometry is in theory currentless. However, when conducting real-life potentiometric experiments, there is always some current flowing in the electrochemical cell, as real instruments are non-ideal and have a finite input impedance [59]. This current is typically very small and often on the order of picoamperes, but for long-term measurements it cannot be ignored. This places a restriction on the materials used to prepare a solid contact, as the impedance of the ISE must be significantly smaller than the input impedance of the instrument in order to accurately measure the voltage. For example, a voltmeter must have an input impedance that exceeds the impedance of the electrochemical cell by a factor of more than 100 if an EMF measurement is to be affected to less than 1% by the systematic error resulting from the nonideality of the voltmeter. Transducers with a high double-layer capacitance help limit EMF drifts over time that arise as a result of the small current flowing through the potentiometric cell [60]. For example, good potentiometers have an input impedance of 10^{12} Ω. With this input impedance, the current flowing in the system can be estimated to be, e.g., around 0.2 pA if the voltage generated by the ISE is 0.2 V. If the capacitance of an electrode is on the order of 1.0 mF, as it is for ISEs with colloid-imprinted mesoporous carbon solid contacts [60], it would take approximately 58 days for the potential to drift 1.0 mV if capacitive charging of the ISM/carbon interface were the only cause of potential drift, while it would take just under 1.5 h for a sensor with a 1.0 μF capacitance to drift the same amount. High capacitance values very effectively decrease drift introduced by residual current, but other sources of drift certainly may exist.

3.2 Characterization of Ion-to-Electron Signal Transduction

One technique that may be used to determine whether the phase boundary potential at a solid contact is dominated by capacitance or by a redox reaction is electrochemical impedance spectroscopy (EIS) [59, 61, 62]. EIS data is obtained through application of a sinusoidal voltage

and analysis of the resulting current. Often, this data is interpreted using a Nyquist plot, which shows, for a wide range of frequencies, the ratio of the voltage and out-of-phase current (i.e., the imaginary or capacitive component of the impedance) versus the ratio of the voltage and the in-phase current (i.e., the resistance, also referred to as the real component of the impedance). In the Nyquist plot, the presence of a large capacitance is indicated by a nearly vertical line in the range of low frequencies (see Figure 7A). This can be used to calculate the low-frequency capacitance of a solid-contact system, which can be very large when using high surface area transducers that provide capacitive signal transduction. Another often observed feature in Nyquist plots is a semicircle in the higher frequency region, which corresponds in the equivalent circuit to a resistance and capacitance in parallel, resulting from the bulk resistance and geometric capacitance of the ISM, respectively (see Figure 7B). It often falls into the same frequency domain as the impedance at the interface between the ISM and underlying electrode and the impedance between the sample solution and the ISM, but because the interfacial impedances are typically much smaller than the impedance of the ISM, they often cannot be observed in well-functioning solid-contact ISEs [63, 64]. However, the Nyquist plot may exhibit a semicircle caused by this interfacial impedance in the case of sluggish electron transfer across that interface [65].

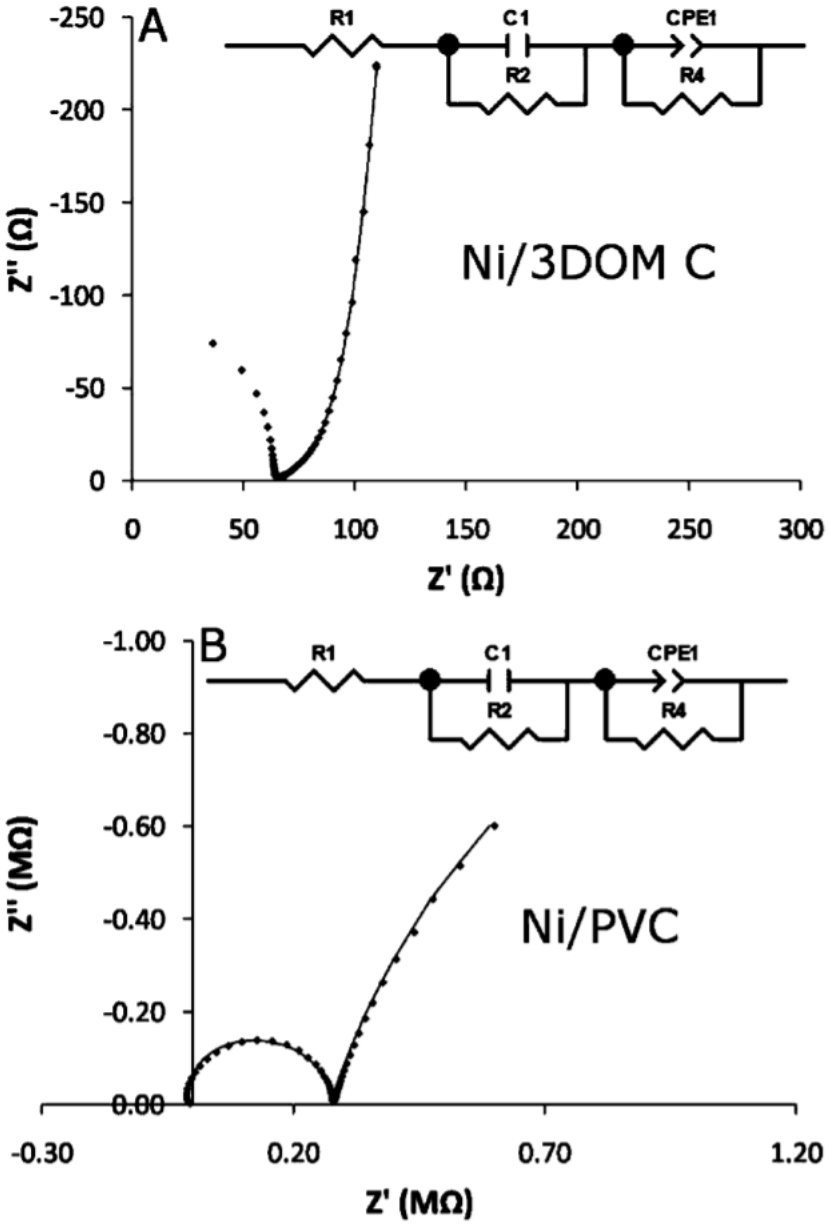

Figure 7. Nyquist plots of (A) 3-dimensionally ordered macroporous carbon and (B) a plasticized PVC membrane on a Ni mesh electrode. Part (A) shows the low-frequency nearly vertical line resulting from the large interfacial capacitance at the surface of the carbon. Reproduced with permission from reference 66.

It is important to distinguish between semicircles associated with the bulk ISM and semicircles associated with interfacial impedance, as erroneous conclusions have been reported in the literature. Notably, there are straightforward experiments that can be performed to avoid such pitfalls. Semicircles associated with impedance at the interface of samples and the ISM have a characteristic dependence of the semicircle diameter on the sample concentration, and semicircles associated with the bulk ISM have a characteristic dependence of the semicircle diameter on the thickness of the ISM layer [67]. Comparing impedance spectra of systems prepared with and without a solid-contact transducer can also give insight into the nature of charge transfer at the interface between the membrane and underlying electrode [68]. For an in-depth discussion of EIS applied to ISEs and a variety of other electrochemical systems, the reader is referred to sources focused on the subject [59, 61, 62].

In addition to EIS, chronopotentiometry and cyclic voltammetry can also be used to measure the capacitance of solid-contact materials. In chronopotentiometry, a constant current is applied, and the resulting potential is monitored, after which the direction of the current is reversed. The magnitude of the drift in potential over time will depend on the capacitance of the solid contact, according to the equation $\Delta E/\Delta t = i/C$, where i is the applied current and C is the capacitance of the electrode [69]. Smaller potential drifts therefore indicate a larger capacitance. Cyclic voltammetry can be used to measure the capacitance of solid contacts by sweeping the potential in the absence of any redox-active compounds, resulting in a relatively constant, capacitive current. In a potential sweep experiment, the capacitive current is equal to $I_c = nFAvC$ where C is the specific capacitance of the electrode surface and v is the potential scan rate [70].

A few studies have looked at transduction mechanisms using such techniques as synchrotron-radiation X-ray photoelectron spectroscopy and near-edge X-ray absorption fine

structure. With these techniques, the location of a chemical species can be determined with very high spatial resolution. For example, it was possible to show that the transduction mechanism at POT-based solid contacts takes place through a surface-based oxidation/reduction reaction [71]. The POT^+ and corresponding lipophilic doping anions were present only in the surface region of the POT in contact with the ISM, even after application of 1.3 V vs Ag/AgCl for one hour. Similar experiments including X-ray photoelectron spectroscopy and valance band spectroscopy were also carried out on multi-walled carbon nanotube (MWCNT) transducers and confirmed the presence of an electrical double layer at the interface [72].

3.3 Calibration-Free Sensing and Redox-Active Transducers

Only shortly after the introduction of coated-wire ISEs [15], experiments with Ag and a mixture of Teflon and graphite as the solid contact were performed. The response of these sensors was interpreted to rely on the formation of O_2/H_2O redox half cell at the membrane/electrical contact interface. However, the electrode-to-electrode standard deviation of E^0 was on the order of 30 mV [73], a range often also observed for coated-wire ISEs without a redox couple or other transducing material controlling the phase boundary potential. A better controlled redox buffer system used a silver epoxy substrate covered with an ion-selective membrane doped with a Ag^+ ionophore [74]. With a 0.07 mV/h drift over ~15 h after a 10 h conditioning period and a standard deviation of the potential as low as 2.7 mV for Na^+ ISEs, this setup performed remarkably well, although there was a concern that in the presence of an ionophore for a primary ion other than Ag^+ the Ag^+ might exchange with the sample for the primary ion, resulting in EMF drift. Indeed, longer term EMF drift was not reported, as is also true for many other reports from the 1990ies and earlier. This is reflected in Table 2, which lists performance characteristics of solid-contact ISEs with redox-active transducers for which either

the E^0 reproducibility or long-term EMF drift was reported. The majority of entries in this table are from the past ten years, illustrating the recent interest in continuous monitoring and the reduction in the frequency of recalibration. As the following discussion of representative examples of solid-contact ISEs with a redox-active transducer shows, the current state-of-the-art lies at an E^0 reproducibility and EMF drift of approximately 1 mV and 10 μV/h, respectively. Only few reports fulfill both criteria.

Table 2: Performance Characteristics of Redox-Active Transducers

Transducing Material	E^0 Standard Deviation (mV)	Drift	Comments	Reference
Ag/Teflon/graphite	~30	NR	NA	73
Ag epoxy	3.7	0.07 mV/h over ~15 h	NA	74[74]
POT	1.3	10 μV/h over 8 days	NA	75[75]
POT/TCNQ	6	0.1 mV/h	Optimized by prepolarization	76
PEDOT/TPFPB$^-$	3.7	0.83 μV/h over 28 d		44
PEDOT-F/TPFPB$^-$	3.0	56 μV/h over 1 d	NA	30
PPy/ferricyanide/ferrocyanide	NR	<42μV/h	NA	77
PPy/graphene	NR	28 μV/h	NA	78
PPy/PFOS$^-$	0.7	NR	Optimized by prepolarization	24
PANI nanoparticles	1	0.7 mV/h over 10 h	NA	79
PANI	0.9	NR		80
N-[2-(phenylamino)ethyl]-methacrylamide polymer	1.9	83 μV/h over ~90 d	NA	81
Tetrathiafulvalene/TCNQ (not a redox pair)	0.9 (NO_3^-), 2.1 (K^+)	17.1 μV/h (NO_3^-), 18.7 μV/h (K^+) over 72 h	NA	82
Poly(vinylferrocene)	NR	NR	Drift only slightly worse than for corresponding IFS electrodes	83
Ferrocene-based SAMs	10	46 μV/h over 40 d	*a*	84
Co(II/III) tris(phenanthroline)	0.7	NR	1.0 mV SD after 7 d, for ion-exchange electrodes	85
Co(II/III) tris(C_9,C_9-bipy)	0.7	NR	Performance loss in few d	86
Co(II) porphyrin/Co(III) corrole	0.7	NR	Not a redox buffer	87
Screen-printed carbon with ferri/ferrocyanide	2.5	NR	Not a 1:1 ratio, maximum E^0 stability 24 to 36 h	88

			into conditioning in O_2-free solution	
AuNPs w/ thiol SAM	0.8	NR	E^0 SD of 1.2 mV after 42 d	89
AuNPs w/ thiol SAM in ISM	NR	12 µV/hover 20 h	NA	90
AgCl/trihexyltetradecyl-phosphonium chloride	1.9	5.9 µV/h between days 3 and 30	No ionophore	91
Ag NPs, AgX	0.1	NR	Stable E^0, slope after 14 d	92
$LiFePO_4$	2.0	1.1 µV/h	NA	93
Ni-based Prussian Blue analogues	1.0(Ca^{2+}), 2.2 (Na^+), 2.4 (K^+)	NR	Stable over several months	94

[a] Optimized reproducibility was with a different transducer than for optimized drift
NR: Not reported. NA: Not applicable.

3.3.1 *Conducting Polymers*

By far the earliest class of transducers to be investigated thoroughly and improved in many iterations were transducers comprising a conducting polymer. The use of conducting polymers as solid-state transducers is attractive because they can be synthesized in many different variations as an additional layer between the sensing membrane and the electrode surface. They also seem an obvious choice considering that suitable transducers require both ionic and electronic conduction and that most conducting polymers attain electronic conductivity upon doping with an ionic additive. These polymers then exhibit electronic conductivity along the polymer backbone, which can exchange electrons with the electrode though redox reactions, while the dopant ions exchange at the interface with the sensing membrane [4, 69, 75]. Conducting polymer-based solid-contact ISEs have been reviewed in depth previously [4, 49, 69, 95]. This review does not attempt to discuss this topic comprehensively, but instead focusses on

the extent to which solid-contact ISEs can be considered calibration-free, based on performance characteristics reported in the literature.

The relative contributions of ionic and electronic conductivity to the total conductivity is a topic rarely discussed in the ISE literature, although a robust literature on this topic exists outside of this field [96, 97]. However, the ionic conductivity of the conducting polymer layer has a profound influence on the performance of a solid contact based on a conducting polymer, as evidenced by the large decrease in capacitance when an ISM is applied to PEDOT as the conducting polymer transducer [69]. The mobility of ions in the conducting polymer and the ease with which ions from either the conducting polymer or ISM phase can transfer into the neighboring phase critically affect the interfacial capacitance. This affect is discussed in more detail below [98].

3.3.1.1 Polypyrrole

The first example of an ISE with a solid contact consisting of a conducting polymer used partially oxidized PPy as the transducing layer, with BF_4^- as the dopant ion [20]. An E^0 standard deviation was not reported but a thorough discussion was provided, explaining how the solid-contact material is able to provide a thermodynamically well-defined interface with both the sensing membrane and the electrode. It was proposed that tetrafluoroborate anions are shared between the PPy and ISM. Possible loss of this relatively hydrophilic anion from the membrane into aqueous samples in exchange for primary ion transfer into the ISM, as it may be relevant to EMF drift, was not considered. Subsequently, improvements in the performance of PPy solid contacts were obtained in several ways. Doping with a combination of ferrocyanide and ferricyanide resulted in an EMF drift of less than 1 mV per day over a period of ten days [77], and the combination of PPy with graphene resulted in a drift of 0.67 mV/h [78], but in neither

case was an E^0 reproducibility reported. In view of E^0 reproducibility, the best performing PPy solid-contact ISEs comprised prepolarized PPy doped with perfluorooctanesulfonate ($PFOS^-$), providing an E^0 reproducibility of ± 0.7 mV initially, and of ± 3.1 mV after 46 days of storage in solution. As a result of the high hydrophobicity of $PFOS^-$, this material is more hydrophobic than most doped conducting polymer membranes [24]. It has been shown that the hydrophobicity of perfluoroalkayl sulfonates and carboxylates is a result of the cumulative electron-withdrawing effect of the many fluorine atoms, lowering the hydration energy of the anionic group [99]. We note that while PPy solid-contact ISEs appear promising, reports on such electrodes that quantitatively discuss both the E^0 reproducibility and long-term drift are missing.

3.3.1.2 Poly(octylthiophene)

Shortly after the first use of PPy, it was shown that POT can also function as a solid contact [75]. While POT has become a very popular solid-contact transducer and studies using it are numerous, similarly as for PPy, there is a lack of reports on POT solid-contact ISEs that describe both E^0 reproducibility and long-term drift. POT was used in an undoped, semiconducting form, and the charge transfer at the POT/ISM interface was ascribed to a cation-exchange process, suggesting that POT likely functions better as a solid contact for cation rather than anion detection. A standard deviation for E^0 was not reported, but the in-batch reproducibility for multiple Ca^{2+} selective electrodes at a particular Ca^{2+} concentration was as low as ± 1.3 mV [75]. Interestingly, as a result of differences in the ease of water layer formation, stabilities of solid-contact ISEs were shown to be better with a solution-cast POT layer as compared to ISEs with an electropolymerized layer [100]. Solution-cast POT used to detect Cl^- was also shown to result in stable potentials, although device-to-device reproducibility and electrode drift were not quantified [101].

POT and polyaniline (PANI) were also used as transducers freely dissolved in the membrane itself, as opposed to a discrete separate layer between the ISM and the underlying electron conductor [16]. This setup showed a good potentiometric response with no response to redox-active species in solution when a low concentration of the conducting polymer in the membrane was used, though here too E^0 standard deviations were not reported. Electrochemical impedance spectroscopy was used to confirm that the dissolved conducting polymer reduces the overall charge-transfer resistance as compared to sensors without conducting polymer [68]. Potential measurements with solid-contact ISEs comprising a POT layer doped with the redox-active 7,7,8,8-tetracyanoquinodimethane (TCNQ), in both its neutral and anionic forms, were characterized by a standard deviation of E^0 of ± 6 mV, a considerable improvement over the ± 36 mV obtained without inclusion of the redox active dopant, although not quite as low as for some other solid-contact systems [76]. With prepolarization resulting in a TCNQ/$TCNQ^-$ ratio of approximately 1:1, the POT/TCNQ electrodes were observed to have a drift of 0.1 mV/h, compared to ~1.4 mV/h for electrodes with POT only. This result is expected, as the TCNQ/$TCNQ^-$ redox couple has a more well-defined redox potential than POT does, and the inclusion of the redox couple should more efficiently buffer the potential. See Section 3.3.2 for a discussion of redox buffer theory.

Clearly, the physical nature of the interface between a solid-contact layer and the ISM is extremely important. As recently as 2018, Michalska's group showed that solution-cast POT does intermix with PVC sensing membranes in the process of the sensor fabrication and during the conditioning of the sensing membranes. The tetrahydrofuran used as the solvent for membrane deposition dissolves the POT layer that is already in place, resulting in a significant amount of POT transferring into the PVC phase (see Figure 8). Changes in the oxidation state of

POT and interaction of POT with other membranes components, such as ionic sites, can alter a sensors' performance [31]. It is possible that similar effects occur with other conducting polymers. Perhaps irreproducibility of this mixing process limits the standard deviation of potentials at this interface. Further work by Michalska's group on a composite transducer material consisting of POT and MWCNTs showed that the interaction of POT with MWCNTs inhibited the transfer of POT into the ISM and resulted in partial oxidation of the POT in the composite layer (see Figure 9) [102].

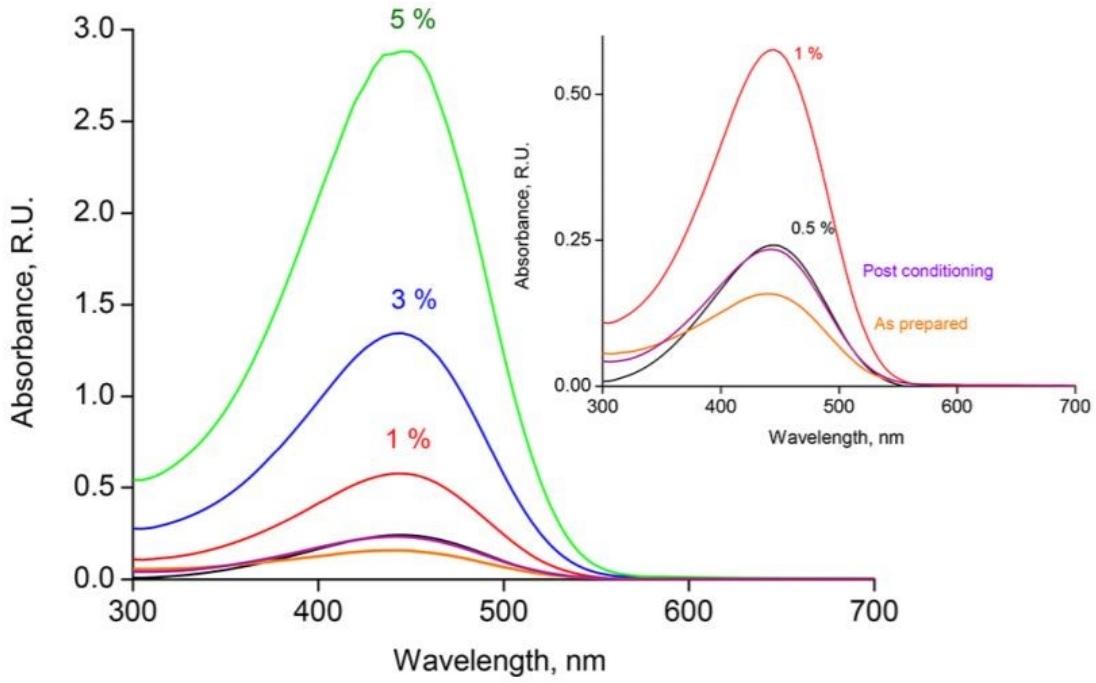

Figure 8. Evidence for transfer of solution-cast POT into PVC membranes. UV–vis absorption by POT clearly increases after the PVC membrane cocktail is exposed to a POT-based solid contact for 14 h. Reprinted with permission from reference 31.

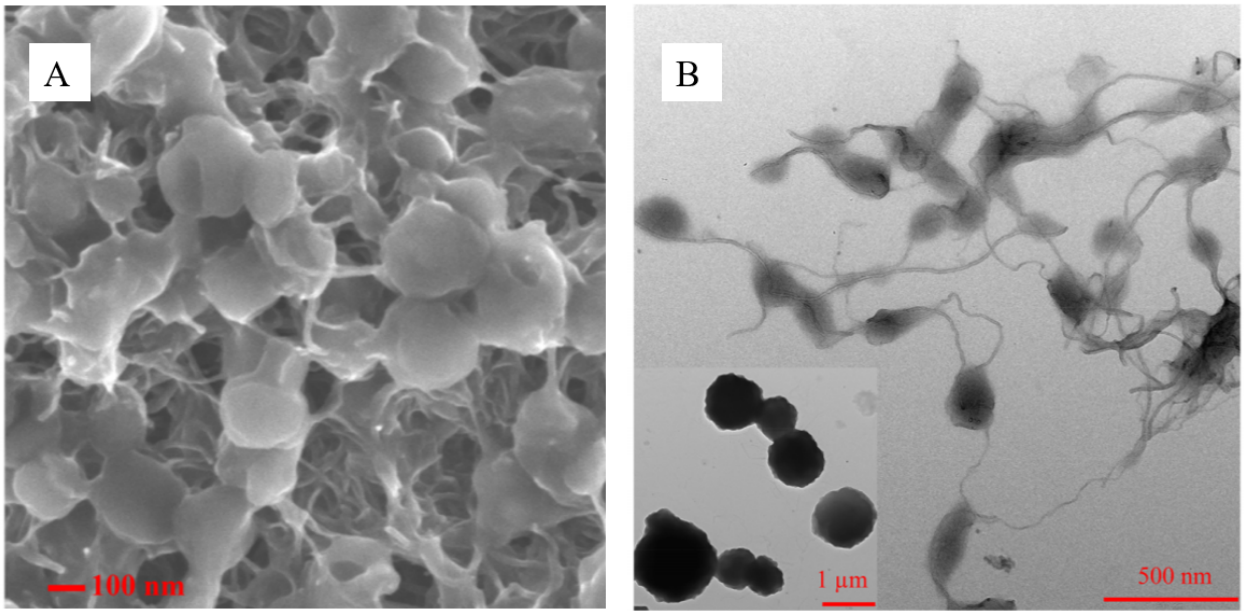

Figure 9. (A) Scanning electron micrograph and (B) tunneling electron micrograph of POT/MWCNT composite material. Inset shows the corresponding image of POT in the absence of MWCNTs. Adapted with permission from reference 102.

3.3.1.3 Polyaniline

Besides electrodes with PANI freely dissolved in the ion-selective membrane (see above) [16], ISEs with a distinct PANI layer as transducer have also been investigated. While earlier work with PANI nanoparticles did not comment on E^0 reproducibilities [103, 104], more recent work reported a value of ± 1 mV, a constant response slope over the course a month, and a drift of 0.7 mV/h over 10 h [79]. PANI/poly(methyl methacrylate) mixtures deposited by electrospinning showed a higher capacitance of 84.7 µF, as compared to the 4.7 µF for the same mixture deposited by drop-casting [105]. A direct comparison between PANI and carbon nanotubes (CNTs) showed E^0 ± 0.9 mV for a PANI layer and ± 1.1 mV for CNTs. The CNT electrodes showed a stable slope after continuous use for 60 days, while PANI electrodes lasted only for 45 days [80]. However, the ultimate limitation for the long-term use of PANI-based

electrodes is probably partial conversion of its conducting into its non-conducting form over periods of several months, a consequence of its pH sensitivity [106].

3.3.1.4 Poly(ethylenedioxy thiophene) (PEDOT)

In recent years, there has been much interest in using PEDOT and its derivatives as a transducer. PEDOT modified with a 14-carbon hydrophobic side chain and doped with tetrakis(pentafluorophenyl)borate (TPFBP) achieved E^0 standard deviations as low as ± 3.7 mV, with a drift of 0.02 mV/day for pH electrodes between day 3 and 31, and a ± 0.1 mV standard deviation for a batch of electrodes measured in a single solution [44]. Vanamo and Bobacka showed that it is possible to adjust the E^0 of solid-contact ISEs with PEDOT(PSS) as the transducer using application of a voltage or current, although drift in the open circuit potential following this adjustment of the solid-contact redox state could not be avoided [107]. Short-circuiting the ISEs to a double-junction Ag/AgCl reference electrode also works for this purpose and has the advantage of an instrument-free setup, but here too drift following the short circuit treatment is apparent. Short-circuiting multiple electrodes did bring their potentials closer together, but the standard deviation of E^0 after days or weeks following this process was not reported [108].

PEDOT derivatized with perfluorooctyl side groups (PEDOT-F) and doped with $TPFPB^-$ showed an E^0 standard deviation of ± 3.0 mV after prepolarization. It was found that before deposition of the ISM the solid contact had an E^0 reproducibility of ± 0.5 mV, providing support that the effect of the ISM should not be ignored. The drift was lowest during the first day of conditioning (56 μV/h), but it should be noted that this low level of EMF drift was achieved with a prepolarization potential that differed from the one that gave the lowest standard deviation of E^0. After 49 days of testing, the standard deviation of E^0 was ± 5.5 mV, and the drift remained

largely unchanged at 50 μV/h [30]. This PEDOT derivative provided a better reproducibility than others, with the perfluorinated side chain contributing to a high hydrophobicity.

The capacitance of the PEDOT surface decreases substantially when an ISM is applied to the conducting polymer. Studies performed to explain this observation found that more mobile ions and a higher ionic content of the ISM increase the observed capacitance [98]. Although reproducibility was not explicitly investigated in that study, it was shown that the choice of underlying electron-conducting substrate and the thickness of the PEDOT(PSS) film influence the conditioning time, and that the biggest contribution to the potential drift of such solid-contact ISEs is likely related to processes at the interface between the solid contact and the ISM [46].

3.3.1.5 Other Conducting Polymers

A number of other conducting polymers have also been used as transducers. A polymer prepared from of the bifunctional monomer *N*-[2-(phenylamino)ethyl]methacrylamide, polymerized though both its methacrylamide and aniline groups, has a conductivity of 6.18 S/cm, a value that is slightly higher than for PANI [109]. It was used as a transducer for Ca^{2+} detection with a urethane-based membrane polymerized through UV irradiation, resulting in covalent bonds between the two polymer layers. This gave devices with an E^0 standard deviation of ± 1.9 mV, with a 3 mV/decade decrease in response slope after three months of use, and a 2 mV/day drift of E^0 [81]. Polyazulene, electropolymerized to contain PF_6^- as the dopant anion and prepolarized to a partially conducting form, provided for a standard deviation of measured potentials of ± 0.9 mV after 30 h of conditioning, an improvement over the ± 3.1 mV upon initial contact with solution. This was an improvement over the chemically polymerized POT used for comparison in the same study, which provided for an E^0 standard deviation of ± 7.9 mV [110].

3.3.2 *Molecular Redox Buffers and Related Redox Systems*

Already in 1995, it was pointed out that a mixture of ferrocene redox states is needed to gain stability of the interfacial potential at a ferrocene-modified surface of the electron conductor underlying an ISM [83]. For that purpose, poly(vinylferrocene) was potentiostatically oxidized half-way. The average EMF drift, reported as peak-to-peak deviation over a 20 day period, was found to be 14.3 mV for solid-contact electrodes compared to 9.9 mV for conventional electrodes [83]. Studies conducted on plasticized PVC membranes containing ferrocene covalently attached to the PVC polymer chain showed that only a small portion of the total ferrocene groups are electrochemically accessible [111]. It should also be noted that the ferrocenium cation is known to be unstable in the presence of molecular oxygen [112]. A separate investigation of poly(vinylferrocene) films on platinum electrodes showed that the conductivity of this polymer is in the range of 10^{-4} S/cm [113]. In comparison, the conductivity of PEDOT can vary widely depending on the production method, but standard PEDOT(PSS) has been measured to have a conductivity of approximately 1 S/cm [114], and while the conductivity of PANI is highly dependent on the acid used to protonate the polymer, it is generally in the range from 1 to 12 S/cm when protonated using common inorganic acids [115].

3.3.2.1 Redox Active Self-Assembled Monolayers

Self-assembled monolayers (SAMs) with fullerene and tetrathiafulvalene as redox-active groups, anchored to gold surfaces by reaction with thiol groups, have also been shown to decrease EMF drift [18]. Further development of this technique was able to show E^0 standard deviations as low as ± 10 mV, and it was suggested that this was the result of a controlled ratio of the oxidized and reduced states, although in this case it was not a 1:1 ratio [116]. Other groups

also investigated redox-active monolayers that contained ferrocene groups as the redox-active constituents. E^0 reproducibility of the final setup was also reported, but even the best-performing sensors, containing a two-carbon alkyl spacer between the thiol and ferrocene groups only achieved a standard deviation of ± 10 mV, while in terms of long-term stability, a different type of SAM containing aromatic spacers between the thiol and ferrocene groups performed the best, with 46 μV/day drift estimated from a 40 day experiment [84]. The ferrocene-modified SAM was able to prevent the formation of an internal water layer forming in between the membrane and underlying electrode, preventing EMF instability and sensitivity to CO_2 [117]. Further improvements of solid-contact ISEs with redox-active self-assembled monolayers as transducers are inherently limited by the small redox capacitance of a single monolayer unless the underlying electron conductor has a large surface area, as is, e.g., the case for porous electrodes.

3.3.2.2 Molecular Redox Buffers

While the redox couple quinone/hydroquinone was covalently anchored to graphite and the ratio of the reduced and oxidized redox groups was shown to affect the observed response, the reported data showed potentials of several electrodes from one batch drifting apart within minutes, and E^0 reproducibility was not reported [118]. The hydroquinone/quinone couple was also incorporated into hydrogel layers, and no significant differences of the resulting electrodes as compared to electrodes with Ag/AgCl inner contacts were reported [119]. It should be noted though that the redox potential of the quinone/hydroquinone couple depends inherently on the local hydrogen ion activity, which might cause EMF drift if samples with volatile acids or bases are analyzed. The long-term effect of CO_2 has not been studied.

The first deliberate attempt to use a hydrophobic redox buffer with a well-defined pH-independent redox potential was based on Co(II) and Co(III) phenanthroline complexes as redox

couple, directly added to an ion-sensitive membrane with ion exchange sites but no ionophore. As a first, the ratio between oxidized and reduced states, Co(II) and Co(III), was shown to control the value of E^0, and a 1:1 ratio resulted in a standard deviation of E^0 of ± 1.7 mV. Using an underlying gold electrode modified with an alkanethiol SAM to prevent water layer formation, the E^0 standard deviation was as low as ± 0.7 mV initially, and ± 1.0 mV after one week [85]. This high stability was achieved because transfer of primary cations into the ISM in exchange for the transfer of the cationic Co(II) and Co(III) phenanthroline complexes into the aqueous sample solution is unfavorable as the result of the high hydrophobicity of the phenanthroline ligands of the Co(II) and Co(III) complexes. However, use of the same redox couple with ionophore-doped ISMs was not successful because stabilization of primary ions in the ISM by complexation with the ionophore makes ion exchange with the aqueous sample much more favorable and promotes, thereby, the loss of the redox buffer species from the ISM into the sample, resulting in potential drift. To that end, this line of work was continued using a more hydrophobic Co(III/II) complex containing dinonyl-modified bipyridine ligands for Co(III/II) complexation, in combination with the K^+ ionophore valinomycin, resulting in a variability of E^0 as low as ± 0.7 mV after only one hour of exposure to K^+ solution. However, this high reproducibility was lost upon longer exposure to solution, as over a few days the redox buffer was still able to leach into the aqueous solution in exchange for primary ions, apparently as the result of the very high stability of the K^+ ionophore complex and the fact that two or three K^+ ions can enter the ISM in exchange for one Co(II) or Co(III) leaving into the aqueous sample, respectively [86]. Further developments of this approach lie in the covalent attachment of the redox buffer to a polymer or use of redox-active complexes of lower charge, the latter both

lowering the hydrophilicity but also decreasing the net free energy of transfer that results from a smaller number of primary ions entering the ISM for each redox-active complex leaving it.

An adaptation of this concept was attempted by fabrication of ISMs doped at the same time with two cobalt complexes that do not represent a redox pair, that is, a Co(II) porphyrin and Co(III) corrole complex that each have a zero net charge. When used along with MWCNTs in the transducing layer, this pair provided for a E^0 standard deviation of ± 0.7 mV, with a deviation of ± 0.80 mV for the same sensor calibrated four times on the same day [87]. Long-term drift was not discussed with much detail. Although these sensors functioned well, the absence of a well-defined redox potential from a redox pair at the interface between the electrode and ISM means that the buffering capacity is low, raising concerns that the long-term stability of the EMF may be limited.

This was pointed out in a publication that introduced the theory of ISEs with a redox buffer solid contact and showed how in a system without a true redox buffer even small concentrations of redox-active impurities crucially can affect the observed E^0 [120]. Figure 10 illustrates the difference between the use of a true redox couple and the combination of a reduced and oxidized species that are not a redox couple and do not react with one another to any significant extent. The dashed line in Panel A shows the well-known shape of a redox titration resulting when the oxidized species $\mathbf{1}_{ox}$ is added to the reduced species $\mathbf{2}_{red}$, resulting in the formation of $\mathbf{2}_{ox}$. Half way to the endpoint of the titration, the ratio of $\mathbf{2}_{red}$ to $\mathbf{2}_{ox}$ is 1:1, and addition of moderate amounts of reductants or oxidants has only a minimal effect on the observed EMF, illustrating the desirable property of a redox buffer. Panel A of Figure 10 also shows the effect of adding $\mathbf{2}_{ox}$ to $\mathbf{1}_{red}$, an experiment equivalent to the Co(II) porphyrin / Co(III) corrole solid contact. The solid line shows that if $\mathbf{2}_{ox}$ contains no impurities of $\mathbf{2}_{red}$, and $\mathbf{1}_{red}$

contains no impurity of $\mathbf{1}_{ox}$, the potential is remarkably independent of the ratio of $\mathbf{2}_{ox}$ to $\mathbf{1}_{red}$. However, even a very small impurity of $\mathbf{2}_{red}$, $\mathbf{1}_{ox}$, or any redox-active species that reacts with $\mathbf{2}_{ox}$ or $\mathbf{1}_{red}$ will affect the observed EMF with the extreme sensitivity characteristic to the endpoint of the redox titration. This also suggests that E^0 values may not be repeatable when reagents from different suppliers or possibly even from different batches of the same supplier are used, as these reagents may then contain different concentrations of impurities.

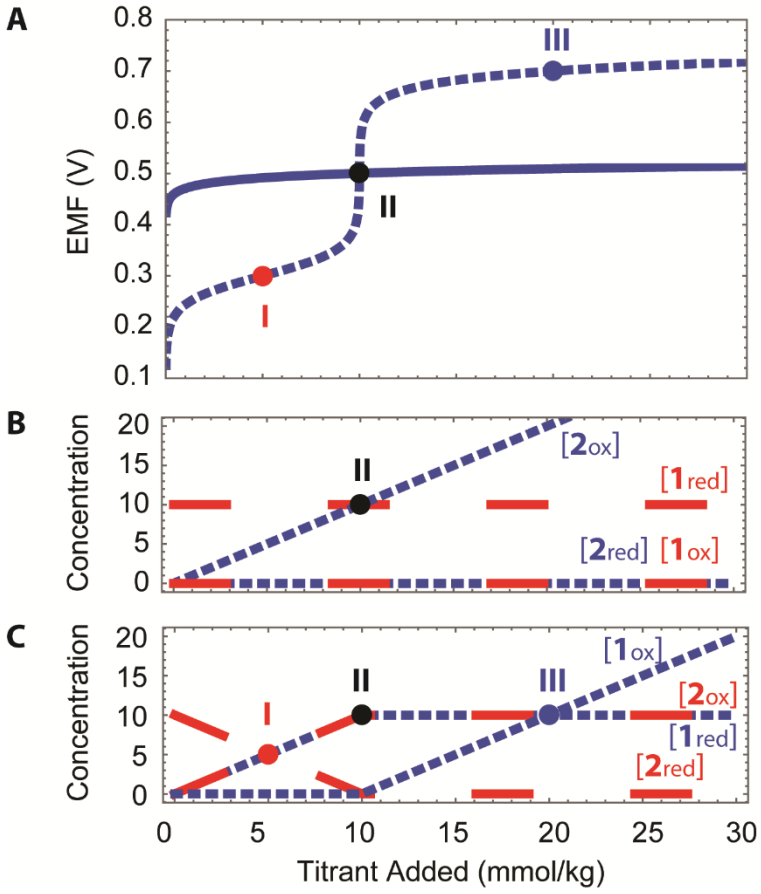

Figure 10. (A) Comparison of the potential arising from the addition of $\mathbf{2}_{ox}$ to $\mathbf{1}_{red}$ (10 mmol/kg, solid line) and a redox titration of $\mathbf{2}_{red}$ (10 mmol/kg) with $\mathbf{1}_{ox}$ (dashed line) for two redox couples with standard redox potentials differing by 0.4 V, $n_1 = n_2 = 1$, and T = 298 K. (B) Species concentrations in the system corresponding to the solid line in Panel A. (C) Species

concentrations corresponding to the redox titration shown as dashed line in Panel A. Reprinted with permission from reference 120.

An approach conceptually analogous to the use of the Co(II) porphyrin / Co(III) corrole pair used the tetrathiafulvalene (TTF) radical cation and TCNQ radical anion, giving an E^0 standard deviation of ± 2.1 mV for K^+ as the primary cation of an ionophore-doped ISM and ± 0.9 mV for NO_3^- for an ionophore-free anion exchanger electrode, with 18.7 μV/h and 17.1 μV/h drift, respectively, over a 72 h period. While the observed drifts are remarkably low, the same concerns as mentioned for the Co(II) porphyrin / Co(III) corrole system apply. The $TTF^{+\bullet}/TCNQ^{-\bullet}$ provides for a low resistance but not a well-defined redox potential, as a redox buffer does, and longer-term experiments have not been reported [82].

A similar approach used screen-printed transducer layers consisting of carbon doped with potassium ferrocyanide. The electrode characteristics were monitored over the course of a 48 h conditioning time. Although no ferricyanide was intentionally included, the authors estimated that the ferrocyanide to ferricyanide ratio was 6.9 to 1. Exposure to oxygen-containing sample solutions, as well as water flux through the ISM to the solid contact, were found to have a detrimental effect on the reproducibility and stability of the electrodes. However, electrodes conditioned in an oxygen-free solution showed an E^0 standard deviation of ± 2.5 mV, taking into consideration five separate calibrations over the time period of 24 to 36 h after the start of conditioning, a time period also found to provide maximum E^0 stability [88].

3.3.3 *Inorganic Redox Buffers and Intercalators*

3.3.3.1 Gold Nanoparticles

Besides conducting polymers and molecular redox buffers, several other types of redox-active transducers have been used in solid-contact ISEs. For example, gold nanoparticles present in two different oxidation states, covered with thiol monolayers and with tetraphenylborate as counterions, were reported to provide an E^0 standard deviation of ± 0.8 mV on initial calibration, increasing to only ± 1.2 mV after six weeks [89]. Conceptually intriguing, this approach has been found difficult to reproduce [121] and may be limited by its comparatively low redox buffer capacity. Gold nanoparticles with hexanethiol monolayers on the surface were also used as dispersions in the ISM, resulting in a drift of 12.9 μV/h over a 20 h period [90]. Unfortunately, little else was reported with which this system could be compared to others.

3.3.3.2 Ag/AgCl

A number of efforts to use ISM-coated silver halides as transducers for solid-contact ISEs have been made over several decades. In a very early study, AgI was coated onto graphite doped with iodine, resulting in systems that required conditioning for over three days [122]. Interesting studies of electrodes with a Ag/AgCl transducer covered with an ionophore-containing membrane using X-ray microanalysis showed that both K^+ and Na^+ ionophores interacted with Ag^+, causing Ag^+ to diffuse through the ISM and to contribute to long-term drift [123, 124]. This effect was prevented using a hydrogel layer between the AgCl layer and the ISM. In view of more recent work with ISEs with internal hydrogel layers, one may wonder though to what extent osmotic pressure differences cause water fluxes through the ISM membranes of such electrodes, resulting in gradual changes in the concentrations of ions in such hydrogels and, thereby, low level potentiometric drift [125].

Presence of a high chloride concentration in an ISM phase in contact with a AgCl-coated Ag lead enhances AgCl dissolution due to the formation of $AgCl_2^-$. AgCl-based transduction using the ionic liquid trihexyltetradecylphosphonium chloride in the membrane showed a response to nitrate, without an ionophore, with a potential standard deviation of ± 1.9 mV and drift of 5.9 μV/h over the 3–30 day time frame [91]. Plasticized PVC membranes backed by plasticized PVC layers doped with silver nanoparticles, a silver halide, and an inorganic salt containing the halide and/or the primary ion in an extremely high concentration showed E^0 standard deviations of ± 0.1 mV for K^+ ISEs with a AgBr/KBr transducer, and ± 0.5 mV for Cl^- electrodes with a AgCl/KCl transducer. Unfortunately, other properties of these electrodes were not described quantitatively, but the K^+ ISEs were reported to give a stable E^0 and response slope after two weeks of exposure to solution [92]. For a sensor with AgCl as transducer in contact with an ISM containing trihexyltetradecylphosphonium chloride as ionic site and a nitrate salt of a Co(II) complex with 4,7-diphenyl-1,10-phenanthroline, E^0 standard deviations as low as ± 0.30 mV at nitrate concentrations greater than 10 mM were reported. A potential drift of 0.09 mV/day over a 90-day period was observed. Reported experimental details suggest that the selectivity measurements were biased [25] and that the cobalt complex was not functioning as an ionophore, contrary to the authors' interpretation [126].

3.3.3.3 Intercalation Materials

Another interesting class of transducers are materials capable of intercalating the primary ion. Using lithium intercalation compounds such as lithium iron phosphate present in an intermediate charge state gave an E^0 reproducibility of ± 2.0 mV, with a potential reproducibility of ± 1.5 mV after 42 days in 0.1 M LiCl, the change in potential being only 1.7 mV over this time period and corresponding to a 1.1 μV/h drift [93]. Other work with Prussian Blue analogues

involved intercalation of K^+ into hexacyanoferrate complexes with Cu, Fe, and Ni and intercalation of Na^+, and Ca^{2+} into Ni hexacyanoferrate. All E^0 standard deviations for the nickel intercalation compound were less than 3.0 mV, with Ca^{2+} being ± 1.0 mV, Na^+ ± 2.2 mV, and K^+ ± 2.4 mV (± 2.2 mV with the iron-based intercalation compound). In spite of possible concerns that a water layer might form at the interface to an ionic material, the sensors were reported to give stable responses over several months, and potentiometric water layer tests did not indicate the presence of a water layer [94]. Other insertion materials investigated as ISE transducer layers include $LiFePO_4$ for Li^+, $Na_{0.33}MnO_2$ for Na^+, and K_xMnO_2 for K^+, each overlaid by a plasticized PVC membrane doped with a suitable ionophore. The electrodes resulted in a potential standard deviation of ± 1.7 mV for a single electrode calibrated 10 times and showed a significantly reduced drift compared to coated wire electrodes, but detailed EMF drift data were not reported [127].

3.3 Capacitive Interfaces

Many electronically conducting materials with large surface areas have been used as capacitive transducers in solid-contact ISEs. The two most common types of materials used for this purpose are porous carbon materials and nanostructured noble metals. Table 3 overviews the performance of solid-contact ISEs with capacitive transducers for which either E^0 reproducibilities or long-term drifts have been reported quantitatively. It also reports the capacitance of those systems for which such data is available. While some publications report the capacitance in F/g, others report it in F/cm^2. To facilitate comparisons, we have converted the latter type of information to F/g when the necessary information was available. Since the capacitance of a solid-contact material is the key parameter that gives it its electrochemical functionality in these devices, reporting this value is helpful for interpreting the overall

performance. Because the capacitance of a particular device is typically affected by the application of the ISM, we recommend that researchers report the capacitance both before and after ISM deposition, although this may be difficult or impossible depending on the characteristics of a particular device.

Table 3: Performance Characteristics of Capacitive Transducers

Transducer Material	E^0 standard deviation (mV)	Drift	Comments	Capacitance	Reference
3DOM Carbon	NR	11 μV/h	NA	NR	128
CIM carbon	7.3 (0.7 with redox couple)	1.3 μV/h over 70 h	NA	20.5 F/g	60
Pencil graphite on cellulose acetate	4.05	NR	NA	NR	129
Ordered mesoporous carbon spheres	9.1	28 μV/h	NA	52.93 F/g	130
MWCNTs	NR	0.2 mV/h over 5 h	NA	NR	131
Octadecylamine SWCNTs	9.2 (activity NR)	0.19 mV/h over 24 h	NA	184 F/g (with ISM)	132
MWCNTs	0.85 in 1 mM Ag^+	NR	NA	NR	133
Octadecylamine MWCNTs w/ prepolarization	2.5	NR	NA	~1.2 F/g	134
MWCNTs on carbon fiber thread	1.5	0.9 mV/h over 13.5 h	NA	NR	135
Reduced graphene oxide	2.32 at max concentration measured	10 μV/h over 24 h	NA	1.92-14.81 F/cm^2	136
Carboxylated graphene	NR	NR	Repeatability ± 4 mV over 19 d	0.68 mF/g (with ISM)	137
GO with hydrophobic side chains	NR	253 μV/h over 10 h	NA	NR	138

Carbon black	1.1 (behind ISM)	9.3 μV/h (in ISM)	E^0 decreased by 5.9 mV over 42 d	85.8 mF/g (with ISM)	139
Carbon black and Pt NPs	1.4 (K^+) 0.2 (NO_3^-)	8.9 μV/h (K^+) 6.3 μV/h (NO_3^-) over 12 hours	Carbon black and Pt NPs	1.2 mF	140[140]
Defect-free graphene	0.7	0.74 mV/h over 15 h	NA	0.21 mF/cm^2 (no ISM) 1.27 mF/cm^2 (with ISM)	141
3:1 carbon black:graphene with acrylic fluoropolymer	0.1	1 μV/h over 50 h	NA	1.471 mF	142
Carbon black ink	2.3 (Ca^{2+}) 0.5 (Cl^-)	0.6 mV/h over 0.5 h	NA	NR	143[143]
Au NPs w/ octylthiol SAM	<10 (in range of calibration)	NR	NA	80 μF/cm^2 (with ISM)	144
Au/Cu NPs with MWCNTs	2.9 (Ca^{2+}) 3.1 (SO_4^{2-})	NR		39.4 F/g [a]	145
Pt NPs	4.1	NR	E^0 decreased by 450 mV in ≈30 d	82 μF (with ISM)	146
Nanoporous gold	1.3 (E at 10^{-5} M KCl)	425 μV/h over 20 hours	NA	NR	147

[a] Value reported per total grams of both Au/Cu NPs and MWCNTs.
NR: Not reported. NA: Not applicable.

3.3.1 Porous Carbon Materials

Porous graphite rods were used already in the early 1970s as solid contacts for ISEs, but the use of carbon nanomaterials with well-characterized geometries and surface chemistries is a more recent development [21]. The first examples were ISEs comprising three-dimensionally ordered macroporous (3DOM) carbon, which were introduced in 2007. 3DOM carbon has not only a very high surface area, but in its preparation reducing conditions are used. This diminishes

the number of oxygen-containing functional groups such as carboxylic acid and phenol groups, and it inhibits water layer formation at the interface of the ISM and the solid contact. Potential drift using 3DOM carbon solid contacts was reduced to 11 μV/h over a one-month period, which was a significant improvement as compared to other approaches at the time and remains among the best to date (see Table 3). However, electrode-to-electrode reproducibility of E^0 was not yet recognized as an important characteristic and was not reported [128]. The key drawback of 3DOM carbon is the scalability of its production. To that end, colloid-imprinted mesoporous (CIM) carbon was introduced as transducer. It is prepared by imprinting in a manner similar as 3DOM carbon but lacks the ordering of pores characteristic for 3DOM carbon, a feature that is not relevant for ISE characteristics and makes production more labor intensive. CIM carbon solid contacts were shown to have a higher capacitance than 3DOM carbon ones and resulted in electrodes with a ± 7.3 mV deviation of E^0. Addition of a Co(II/III) redox buffer further lowered this standard deviation to 0.7 mV. Without redox couple, CIM carbon electrodes showed a drift of 1.3 μV/h over a 70 h period [60]. Figure 11 shows scanning electron micrographs of both CIM carbon and 3DOM carbon. Ordered mesoporous carbon spheres have also been used, but the E^0 standard deviation of ± 9.1 mV and drift of 28 μV/h over 70 h were not quite as promising [130]. Interestingly, using pencil graphite as transducer and underlying electron conductor on a non-conducting polymeric substrate, an E^0 of ± 4.05 mV was found [129].

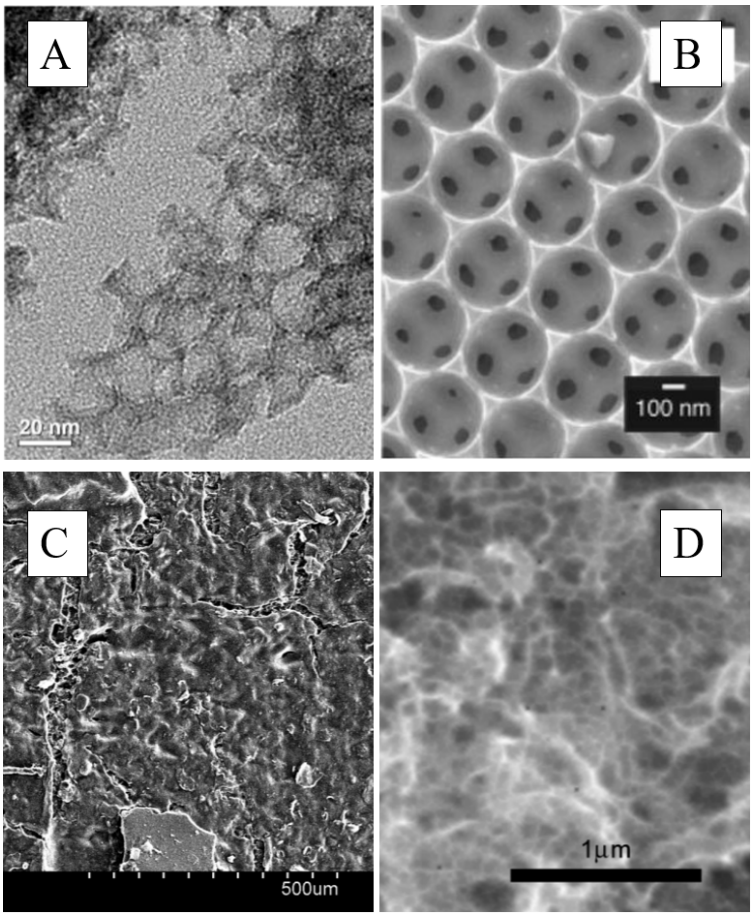

Figure 11. Scanning electron micrographs (SEMs) of (A) CIM carbon, (B) three-dimensionally ordered macroporous carbon, (C) graphene oxide, and (D) SWCNTs. Adapted with permission from references 60, 128, 136, and 148, respectively.

3.3.2 Carbon Nanotubes

The use of imprinted nanoporous carbons as transducers inspired a number of research groups to use other high surface area carbon nanomaterials. Carbon nanotubes (CNTs), both single-walled (SW) and multi-walled (MW), in unmodified and several modified forms have been used extensively as solid-contact materials, although initially CNT-based sensors were not evaluated in view of the criteria important to creating calibration-free sensors. In an early study, for example, it was stated that over 25 days the only performance characteristic with significant

deterioration was the detection limit [148]. (See Figure 11 for an SEM image of this transducer.) Other early work with multi-walled carbon nanotubes showed their effectiveness as transducer, but only the medium-term stability of 0.2 mV/h was reported [131]. Planar, disposable devices with octadecylamine-modified SWCNTs as transducer layer were shown to result in a 0.19 mV/h drift over 24 h, with a potential standard deviation of ± 9.2 mV [132]. A figure of the setup used for these electrodes is shown in Figure 12. Multi-walled CNTs that were modified with three different Ag^+ ionophores showed a stability of ± 0.71 to 1.12 mV over 12 h, with a potential reproducibility for a single electrode in 12 measurements of ± 0.77 to ± 1.37 mV [149]. Similar MWCNT electrodes with a different Ag^+ ionophore resulted in a standard deviation of the EMF of ± 0.85 mV for 50 electrodes immersed in a 1 mM Ag^+ solution [133]. Carbon nanotubes functionalized with octadecyl chains are soluble in tetrahydrofuran and can be deposited as a solution, resulting in more uniform films with a higher capacitance as compared to non-functionalized nanotubes [150]. In an attempt to set the potential of a batch electrodes to the same value, the use of octadecylamine-modified MWCNTs was investigated using both prepolarization and short-circuiting. Short-circuiting for 48 h resulted in a E^0 standard deviation of ± 2.5 mV [134]. Devices with a transducer layer consisting of multi-walled carbon nanotubes dispersed in an ISM deposited on a carbon fiber thread substrate showed a good Nernstian response, with an E^0 standard deviation of ± 1.5 mV after the electrodes were short circuited with a reference electrode overnight, and they exhibited a drift of 0.9 mV/h over 13.5 h [135]. Evidently, many of these CNT-based transducers are able to achieve relatively low E^0 standard deviations, but to date there have been no reports on CNT-based transducers with potential drifts as low as for nanoporous carbon materials.

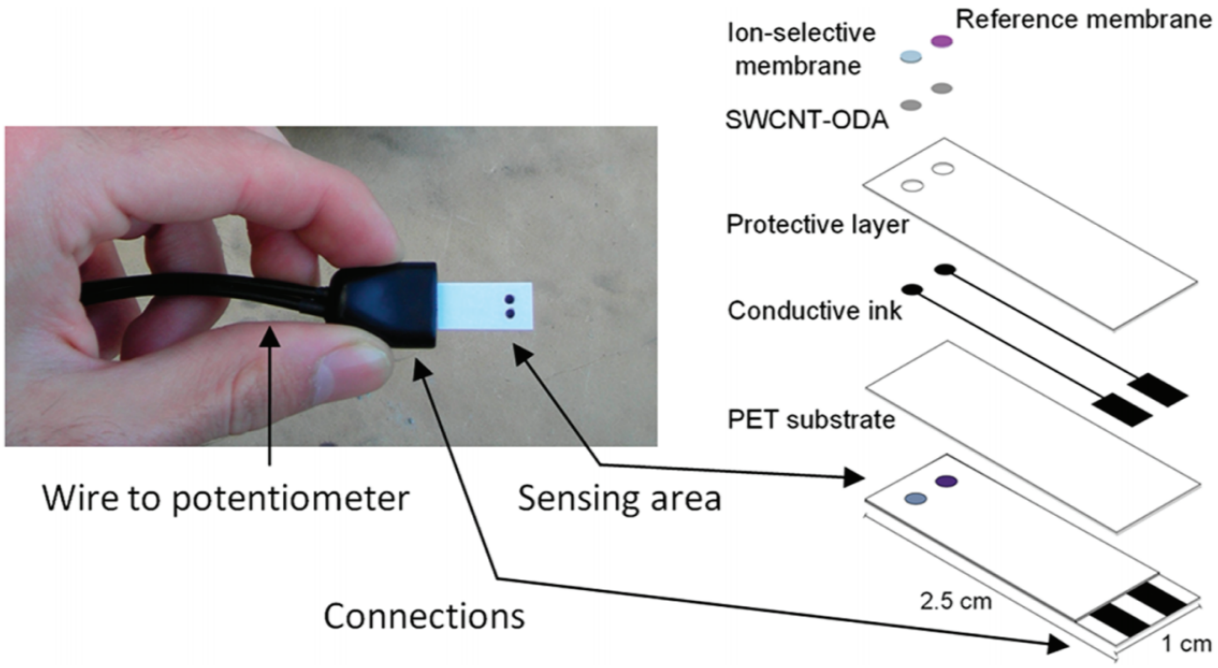

Figure 12. Example of a miniaturized ISE and reference electrode with SWCNT as signal transducer layer. Reprinted with permission from reference 132.

3.3.3 Graphene Oxide and Reduced Graphene Oxide

Reduced graphene oxide (see Figure 11) has also been investigated as signal transducer, with a 10 μV/h drift over 24 h, and a maximum deviation of the response on the linear portion of the calibration curve of ± 2.32 mV [136]. A device comprising several layers of defect-free graphene diminished E^0 to ± 0.7 mV but the drift of 0.74 mV/h over 15 h was relatively large and the response slope for the primary ion K^+ was sub-Nernstian (53.53 mV/decade) [141]. In a comparative study, graphene functionalized with carboxyl groups and deposited as an aqueous suspension showed similar performance to PEDOT, PANI, and POT. Repeatability over 19 days was within ± 4 mV [137]. Graphene oxide modified with hydrophobic alkyl chains was added

directly to ISMs for Ca^{2+} detection, improving the stability of the slope and limit of detection over a two week period, and reducing drift to 253 μV/h over 10 h [138].

3.3.4 Carbon Black

The mesoporous carbon materials, carbon nanotubes, and graphene derivatives that have been used as transducing materials in ISEs are well characterized in terms of chemical composition, geometry, and purity. The same is not true for carbon black, which is a high surface area form of carbon resulting from the incomplete combustion of petroleum products. It comes in various different commercially available forms, designed as pigments and conductors of heat and electrical current. The commercial availability and low price may set off the variability in performance characteristics depending on the supplier. A layer of carbon black (Printex XE-2, BET surface area 910 m^2/g, average particle size 30 nm) as transducer resulted in E^0 standard deviation of ± 1.1 mV, which increased to ± 5.9 mV over the course of 7 weeks. One may wonder whether such performance deterioration results from the presence of residual functional groups comprising oxygen, which are likely present on any high porosity carbon material unless its production or subsequent treatment has carefully avoided surface oxidation. Incorporation of the carbon black as transducer directly into the ISM resulted in a worse initial reproducibility of ± 4.3 mV, but better stability and lower drift at 9.3 μV/h, as well as a higher capacitance of 429 μF [139]. A 3:1 ratio of carbon black (Printex XE-2) to graphene transducer with addition of acrylic fluoropolymer showed an exceptional performance of E^0 SD ± 0.1 mV, with ± 0.02 mV for measurements with a single electrode. The drift was 1 μV/h over a 50 h period but no longer-term experiments were performed [142]. A carbon black ink (BP 2000) acting as transducer on a cotton thread-based electrode was found to provide a E^0 standard deviation as low as ± 2.3 mV for Ca^{2+} electrodes and less than ± 0.5 mV for Cl^- electrodes. At 0.6 mV/h over a 30 min time

period, the drift was rather high, though [143]. Interestingly, devices with a signal transduction layer consisting of a combination of carbon black (Vulcan XC-72) and platinum nanoparticles achieved reproducibilities as good as ± 1.4 mV for K^+ and ± 0.2 mV for NO_3^- ISEs, with 8.2 and 6.3 μV/h drift, respectively, over 172 h. One month of exposure to the conditioning solution resulted in a change of the standard potential by 4.9 and 3.9 mV, respectively [140]. It appears though that this good performance is caused primarily by the carbon black and not the platinum nanoparticles. An image of this transducer is shown in Figure 13.

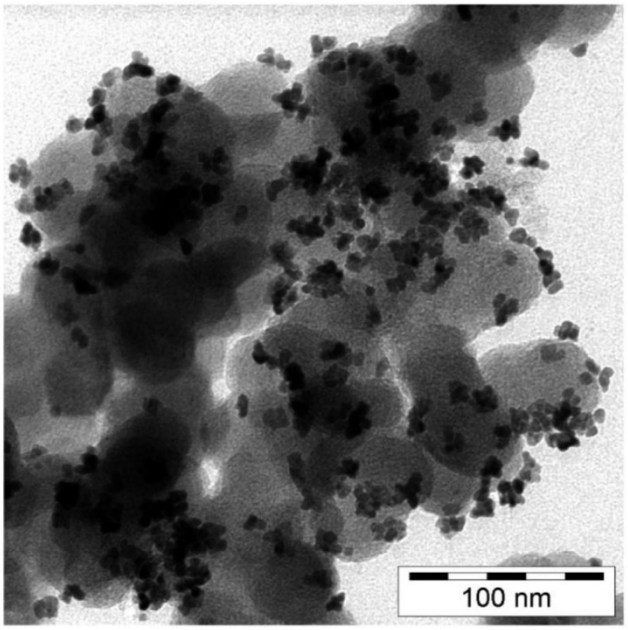

Figure 13. Electron micrograph of a carbon black and platinum nanoparticles composite transducer. Reprinted with permission from reference 140.

3.3.5 Noble Metal Nanostructures

Besides carbon nanomaterials, a range of noble metal nanoparticles have been used to provide for a large interfacial capacitance. In parallel studies, gold nanoparticles with octylthiol groups showed a higher reproducibility when compared to both devices with butylthiol-modified nanoparticles and POT as signal transducers. The standard deviation of potential readings at a set

concentration was less than 10 mV, while same-day recalibration yielded standard deviations of the potential at the same activity in the range ± 0.5 to ± 1.0 mV. Longer-term stability was not assessed, while EIS confirmed the mostly capacitive nature of the interface [144]. Gold nanoparticles with layers of either α-lipoic acid or α-lipoic amide were tested as transducers for Pb^{2+} electrodes. The resulting sensors showed super-Nernstian responses, but the lipoic acid based transducer performed the best, achieving an E^0 reproducibility of ± 3.2 mV after a three-day conditioning process [151]. Composite nanoparticles made of gold and copper combined with MWCNTs were used as a transducer in both Ca^{2+} and SO_4^{2-} ISEs, achieving an E^0 reproducibility of ± 2.5 mV for Ca^{2+} and ± 3.1 mV for SO_4^{2-} [145]. A layer of platinum nanoparticles resulted in a E^0 standard deviation of ± 4.1 mV, although over the course of a month, the actual E^0 value decreased by almost 450 mV [146]. Nanoporous gold was able to reduce drifts to 425 μV/h over 20 h, with ± 1.3 mV being the best potential reproducibility between electrodes at an experimentally measured primary ion concentration (see Figure 14 for an image of the transducer). These electrodes were miniaturized, with a 250 μm diameter gold wire that was modified to form the nanoporous layer on the surface [147].

In summary, while some metal nanoparticles systems provide for rather small E^0 standard deviations, none of these systems has been as successful as the better carbon nanomaterial systems, and often potential drifts were either not assessed or were comparatively large.

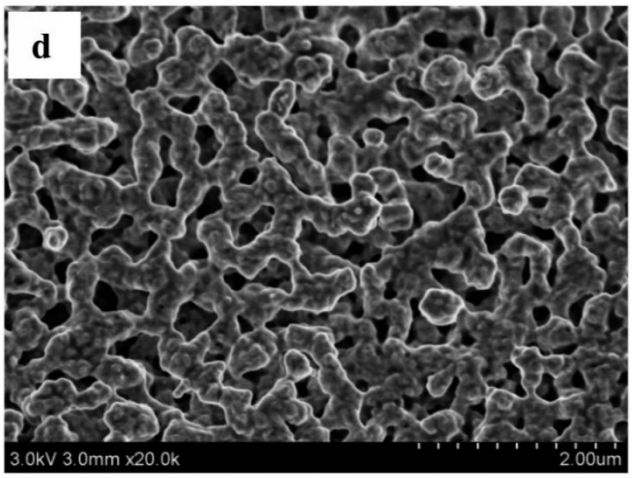

Figure 14. Scanning electron micrograph of a nanoporous gold film used as a solid contact. Reprinted with permission from reference 147.

3.4 Mixed Transduction Mechanisms

It has been proposed that sensors with hybrid transducer materials that combine redox activity with a high double-layer capacitance can possess the advantages associated with both transduction mechanisms. Table 4 summarizes the key performance characteristics of ISEs with such hybrid transducer materials.

Table 4: Performance Characteristics of Mixed-Mode Transducers

Transducing Material	E^0 standard deviation (mV)	Long-term Drift	Comments	Reference
Carbon black and Cu(I) redox polymer	NR	0.18 mV/h over 24 h	NA	152
Graphene and Ag^+TPFPB^-	1.34 in batch, 1.26 inter-batch	1.6 mV/h	NA	153
PANI and graphene	10	NR	NA	154
PEDOT(PSS) and decamethylferrocene	3.9	NR	NA	155
3D porous graphene and mesoporous Pt NPs	2.5	NR	Good response retained after 15 d	156

POT and MoS_2 NPs	NR	~9.0 μV/h over 10 days	NA	157
Tubular gold and tetrathiafulvalene	4.64	NR	E^0 decreased by 5 mV over ≈60 d	158
RuO_2 NPs	2 (H^+)	0.15 mV/h	NA	159
RuO_2 NPs	0.5 (K^+)	85 μV/h over 15 h	NA	160
RuO_2 and poly(3-octylthiophene-2,5-diyl)	1 (for 3 days in a row)	28 μV/h	NA	161
MOF with Ni nodes	NR	11.1 μV/h	E^0 decreased by 15 mV over 25 d	162
CIM carbon and Co(II/III) redox couple	0.7	NR for mixed material	NA	60

NR: Not reported. NA: Not applicable.

A comparative study looking at different transducer layers using various combinations of carbon black, fullerenes, a redox-active polymer based on a polyamide with quinoline groups acting as ligands for copper ions, and a cation-exchanger with benzenesulfonate groups showed that the best reproducibility resulted with a mixture of carbon black, redox polymer, and the ion-exchanger, while long-term stability was maximized with carbon black alone or a combination of ion-exchanger with redox polymer, giving a drift of 0.18 mV/h over a 24 h period. However, many of these transducers showed sensitivity to the concentrations of redox species in solution, and no attempt was made to control the ratio between different redox states of Cu to prepare a redox buffer. Both the minimized long-term stability and the undesirable redox sensitivity were attributed to the presence of carbon black [152].

The use of graphene with nanoparticles of silver tetrakis(pentafluorophenyl)borate located under a standard PVC membrane plasticized with *o*-nitrophenyl octyl ether (*o*-NPOE) and containing valinomycin resulted in an E^0 standard deviation for the K^+ response of ± 1.34 mV in a batch of five electrodes, and ± 1.26 mV between batches, with a drift of 0.18 mV/h over a time period of several hours [153]. Slow dissolution of the nanoparticles in the ISM may have

contributed to this relatively large drift. A three-dimensional porous composite of graphene with dispersed mesoporous platinum nanoparticles showed a E^0 standard deviation of ± 2.5 mV for the detection of Cd^{2+}.The standard deviation of E^0 measured multiple times over a 15 day period was ± 1.6 mV [156]. Paper-based sensors with a hybrid transducer layer consisting of a composite of nanoscale "tubular" structures comprising gold and tetrathiafulvalene exhibited an E^0 reproducibility of ± 4.64 mV initially, and ± 8.21 mV after two months, with a 5 mV decrease in the absolute value of E^0 [158].

A combination of PANI with dispersed graphene resulted in a E^0 standard deviation of ± 10 mV or lower, much better than for PANI alone in corresponding control experiments. Although these results are not exceptional, they give evidence that having a mixture of components with different transduction mechanisms can improve the performance [154]. Mixed transduction was investigated using PEDOT doped with PSS synthesized to contain nanostructured domains with interconnecting pores. Even when these transducer layers were filled with a decamethylferrocene (DMFc)/decamethylferrocenium ($DMFc^+$) redox buffer with a 1:1 ratio of the reduced and oxidized species, the E^0 SD was with ± 3.9 mV still relatively large. It is unclear to what extent this may be related to the fact that while $DMFc^+$ has a higher hydrophobicity than the ferrocenium cation it is still prone to chemical decomposition [112]. For electrodes containing DMFe/$DMFc^+$ in the solid contact, use of plasticized PVC-based ISMs resulted in a sub-Nernstian responses, which was explained by extraction of DMFe/$DMFc^+$ into the membrane phase, while use of a silicone-based ISM resulted in a Nernstian response [155]. A combination of POT and MoS_2 nanoparticles, shown in Figure 15, was used as transducer in ISEs to measure nitrate in soil, and showed good stability at ~9.0 μV/h drift over 10 days and a standard deviation of the potential in a 1.6 mM solution of approximately ± 7 mV [157].

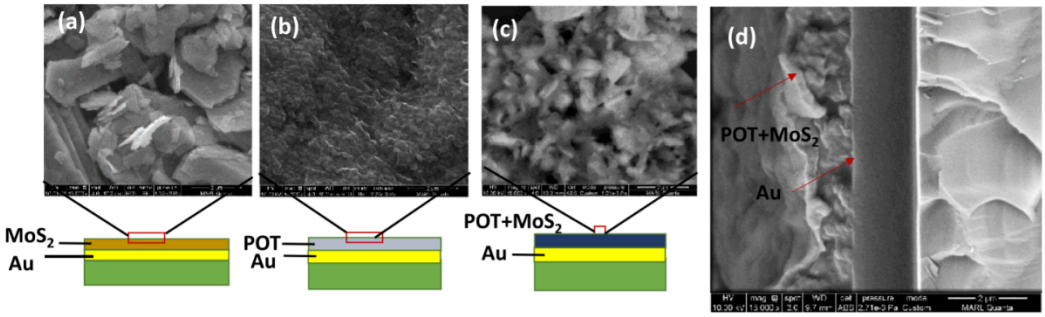

Figure 15. Electron micrographs of MoS_2, POT, and POT/MoS_2 composite transducers. Reprinted with permission from reference 157.

Use of ruthenium dioxide nanoparticles as transducer resulted in a E^0 standard deviation of ± 2 mV for pH electrodes and a drift of 0.15 mV/h over 15 h. This transducer has an especially high capacitance, as high as 1.12 mF [159]. With K^+ electrodes, this same transducer resulted in E^0 ± 0.5 mV and drift of 85 µV/h [160]. A combination of ruthenium dioxide nanoparticles and poly(3-octylthiophene-2,5-diyl) resulted in a capacitance of 3.11 mF, with an E^0 standard deviation of ± 1 mV, not for a batch of electrodes but for multiple calibrations of the same sensor on three subsequent days, and a drift of 28 µV/h [161]. Solid-contact ISEs were fabricated using a metal-organic framework with Ni-containing nodes and showed a change of 15 mV in E^0 over 25 days, with 11.1 µV/h drift for nitrate sensing. The reproducibility of E^0 was not reported [162].

3.6 Miniaturized Reference Half Cells

Although much of the emphasis of this review is on the calibration-free nature of solid-contact ISEs, it is important to recall that an electrochemical cell used for potentiometric measurements consists of both an ISE and a reference half cell. Therefore, efforts aimed at the

development of miniaturizable reference electrodes with highly reproducible half-cell potentials are crucial too for addressing the goals of calibration-free sensing.

In contrast to the ISE, the reference electrode must provide a constant and sample independent half-cell potential. In conventional electrode setups, this is often accomplished through the use of free-flowing, high ionic-strength bridge electrolyte solutions that minimize the liquid junction potential at the interface with the sample. Because salt bridges are difficult to miniaturize, there is much interest in replacing the salt bridge with a material that provides for a steady-state ion distribution between the reference element and the sample to give a sample-independent phase boundary potential.

Three general approaches to replace the conventional salt bridge will be discussed here. These include slow dissolution of a hydrophilic electrolyte from a reference membrane or other device that slows dissolution of the electrolyte, resulting in a phase boundary potential defined in a similar manner as that with a conventional salt bridge, i.e., controlled by the distribution of the hydrophilic electrolyte across the interface of the membrane and sample [44]. Reference electrodes have also been developed where a current pulse results in a well-defined release of ions from a reference membrane, resulting in predictable ion concentrations on both sides of the sample and the reference membrane and, therefore, a well-controlled phase boundary potential [163]. Finally, ionic liquid reference electrodes rely on the distribution of a moderately soluble salt across the interface between a polymer membrane and the sample [164]. The relative concentrations of the ionic liquid across the interface determine the reference potential.

The results of various approaches to these three mechanisms are summarized in Table 5. As the 19 entries in this table illustrate, a considerable amount of work has been performed in this field. Best performances to date are in the range of about 1 mV for the reproducibility of E^0

and a few microvolt per hour for drift, values that are very similar as for the best of the solid-contact ISEs discussed above. However, electrode characteristics in view of calibration-free use have not been reported very consistently. Half of the original publications on solid-contact reference electrodes do not comment on drift, and those that do report drift have studied drift over periods as short as a few hours or as long as three months. Moreover, several reports do not report on E^0 reproducibility at all. This lack of consistency is likely the result of the only relatively recent emergence of the desire to make calibration-free measurements.

It is also interesting to see the type of ions whose concentrations were varied in samples to confirm that the reference electrode did not respond to ion concentrations in the samples. Almost every study reports the effect of Na^+, K^+, and Cl^-, choices clearly driven by the abundance of these ions in biological samples. Interference of H^+ and HCO_3^- has also been tested often, a fact that seems to be largely driven by the desire to confirm that pH sensitive groups of the reference membranes or the underlying transducer do not affect the response of reference membranes. The effect of NO_3^- has been tested quite frequently by those who use ionic liquid-based reference electrodes because this anion is a good representative for ions of low hydrophilicity. In contrast, effects of other ions, such as Li^+, Mg^{2+}, Ca^{2+}, NH_4^+, or Br^-, have been tested much more infrequently.

Table 5: Characteristics of Solid-State Reference Electrodes With Homogeneous and Heterogeneous Reference Membranes

Polymer	Other Membrane Components	E^0 SD (mV)	Drift	Electrical Resistance	Electrode Interface	Type of Sample Interface	Refer-ence
Acrylic acid/ acrylonitrile	Tetramethylammonium chloride	1.1 mV	NR	NR	Iron Oxide, H^+	Miscible liquid junction	165
PVC, plasticized	DOS, Ag, AgCl, KCl, methyltridodecylammonium tetrakis(pentafluorophenyl)borate	Exact number NR	NR	0.7 kΩ	PEDOT(PSS)	Liquid junction	166
PVC, plasticized	*o*-NPOE, Tetrabutylammonium tetrabutylborate	NR	NR	NR	PEDOT	Salt partitioning	167
Poly(butyl acrylate)	Ag, AgCl, KCl, lipophilic salt	As low as 0.2 mV	1.5 mV/h over 5 h	10^5 Ω	PPy(Cl)	Liquid junction	168
Poly(butyl acrylate)	Ag, AgCl, KCl in microspheres, lipophilic salt	NR	Long-term NR	$10^{6.3}$ Ω	POT	Liquid junction	169
Poly(butyl acrylate)	K^+, Na^+, Cl^-, NO_3^-, octadecylamine-SWCNTs	Within 100 mV (intrabatch)	NR	250 kΩ	ODA-SWCNTs	Liquid junction	170
PVC, plasticized	DOS, AgCl (in PPy microcapsule), KCl, methyltridodecylammonium tetrakis(4-chlorophenyl)borate	4.0 mV	NR	10^4 Ω	POT (or Ag/AgCl)	Liquid junction	171
Poly(vinyl acetate)	Solid KCl	NR	Within 2 mV over 71 d	NR	Ag/AgCl	Miscible liquid junction	172
Poly(vinyl-butyral)	AgCl, Ag, NaCl	NR	90 µV/h over 14 h	400 kΩ	Ag/AgCl	Miscible liquid junction	173
PVC, plasticized	DOS, AgBr, Ag, KBr	1.09 mV	Maximum 8.3 µV/h over 10 d	NR	Ag/AgBr	Liquid junction	174
Poly(vinyl-butyral)	KCl on SiO_2	0.5 mV	7.0 mV/h	NR	RuO_2, SiO_2	Miscible liquid junction	175
PVC, not plasticized	KCl	10 mV, batch of 50	Stable over 3 months	<1 MΩ	Ag/AgCl	Miscible liquid junction	176
PVC, plasticized	*o*-NPOE, 1-Methyl-3-octylimidazolium bis(trifluoromethylsulfonyl)imide	NR	42 µV/h over 15 d	NR	3DOM carbon	Ionic liquid partition	177
Fluoro-silicone (Dow RTV 730)	1-Methyl-3-octylimidazolium bis(trifluoromethylsulfonyl)imide	NR	88 µV/h over 8 d	4.7 MΩ	CIM carbon	Ionic Liquid Partition	178[178]

Butyl acrylate/ decyl acrylate	1-butyl-3-methylimidazolium tris(pentafluoroethyl) trifluorophosphate (or 1-hexyl-3-methylimidazolium)	5.0 mV	0.2-0.4 mV/h over 10 h	NR	PEDOT	Ionic liquid partition	179
PVC	*o*-NPOE, Co(II/III) phenanthroline, 1-methyl-3-octylimidazolium bis(trifluoromethylsulfonyl)imide	2.1 mV (carbon rod), 1.5 mV (gold)	0.3 mV/h over 72 h	NR	Co(II/III) phenan-throline	Ionic liquid partition	180
PVC	*o*-NPOE , Co(II/III) dinonylbipyridine, 1-methyl-3-octylimidazolium bis(trifluoromethylsulfonyl)imide	2.8 mV	1.7 μV/h over 110 h	NR	Co(II/III) dinonylbi-pyridine, CIM carbon	Ionic liquid partition	181
Poly(methyl methacry-late)	1-Octyl-3-methylimidazolium bis(trifluoromethylsulfonyl)imide, AgCl	10 mV	154 μV/h over 1 d	630 kΩ	Ag/AgCl	Ionic liquid partition	43
Poly(methyl methacry-late) poly-styrene copolymer	1-Dodecyl-3-methylimidazolium bis(trifluoromethylsulfonyl)imide, AgCl	2.0 mV	0.7 mV/h over 24 h	75-150 kΩ	Ag/AgCl	Ionic liquid partition	182

NR: Not reported.

3.6.1 Solid-State Reference Electrodes with Hydrophilic Electrolytes

In one approach, the common silver/silver halide inner reference element was replaced with a stainless steel rod, which was thermally activated to generate a uniform oxide layer on its surface. This rod is, therefore, pH sensitive, and a reference potential is generated by the encapsulation of this wire into an acrylic acid–acrylonitrile copolymer, which provides a constant hydrogen ion concentration, and also contains a very high concentration of tetramethylammonium chloride as bridge electrolyte to control the interface to the sample. The full reference electrode is not sensitive to the solution pH, and the best reproducibility obtained was ± 1.1 mV. A lifetime of these reference electrodes of 100 days was claimed but long-term drift was not reported [165].

Other efforts to prepare solid-state reference electrodes have used conducting polymers as internal transducers, much like the solid-contact ISEs discussed above. An all solid-contact sensing system was prepared with a solid-state reference electrode consisting of PVC plasticized with *o*-NPOE and doped with tetrabutylammonium tetrabutylborate, with PEDOT as an underlying transducer. This reference electrode was not studied in terms of the electrode-to-electrode reproducibility but did have stable response over a 3-month period, despite a 2-minute equilibration time after sample concentration changes [167]. One study looked at PEDOT and PPy using various doping ions, including perchlorate and PSS. The best performance in terms of redox insensitivity and reproducibility was found with conducting polymer layers doped with PSS, which were covered with a plasticized PVC layer containing solid Ag, AgCl, a suspension of KCl, and lipophilic salts. The authors report a reproducibility on the order of a few millivolts but no numerical values were provided [166]. PPy doped with chloride has also been used as an ion-to-electron transducer behind poly(*n*-butyl acrylate) membranes. Again, the Ag, AgCl, KCl,

and a lipophilic salt were required membrane components. The resistance to various types of interferents was excellent, with slopes less than or equal to 0.9 mV/decade for K^+, Na^+, Cl^-, and NO_3^-, although sensitivity to the ferrocyanide/ferricyanide redox couple was 6.7 mV/decade. The authors emphasized as improvements over the PVC-based membranes the avoidance of plasticizer, which could leach from the membrane into samples, and the fact that these reference electrodes can be prepared in the same manner as the corresponding ISEs [168]. Further improvement on this method was accomplished by introduction of poly(*n*-butyl acrylate) microspheres to contain the solid components. These microspheres were dispersed in a solution of poly(*n*-butyl acrylate) before casting of the reference membranes, and prevented a response to NO_3^- above approximately 0.1 mM that was observed in membranes without microspheres, as well as resulting in more stable potentials on changing KCl concentrations. [169]. Another application of microcapsules was the use of polypyrrole capsules containing either AgCl or KCl in plasticized PVC membranes in which the other salt was dispersed [171]. Electrodes with microcapsules containing AgCl used without POT as transducing layer had a standard deviation of the potential of ± 4 mV for 20 calibrations performed over a period of one month. Poly(butyl acrylate) doped with Ag, AgCl, and KCl has also been used as a reference membrane using octadecylamine-modified single-walled carbon nanotubes, which were used in planar miniaturized solid-contact reference electrodes. These electrodes were not sensitive to solution pH, unless used before being fully conditioned, and were reported not to respond to other ions. These electrodes were not reproducible from one batch to the next, though, resulting in potentials varying by as much as 100 mV, which was attributed to membrane heterogeneity [170]. The potential stability and resistance to sample electrolyte changes of several types of heterogeneous membranes in which silver halide salts were dissolved and membranes containing a lipophilic

salt were compared to several commercially available reference electrodes by Lingenfelter and co-workers [183]. No specific data on electrode-to-electrode reproducibility was reported, but the stability of several systems over a 30 h period was less than 5 μV/h drift.

A poly(vinyl acetate) and solid potassium chloride composite prepared by injection molding with a Ag/AgCl inner contact was stable within 2 mV over 71 days while stored in 3 M KCl, although there was hydroxide interference [172]. A poly(vinyl butyral) (PVB) reference membrane was prepared with Ag/AgCl particles and excess sodium chloride, which had low sensitivity to the tested electrolytes and could be stored dry for a period of up to three months [173]. Over 14 h, the drift was 90 μV/h, although again no data about E^0 reproducibility was presented. PVC membranes loaded with AgBr and KBr with some metallic Ag present were able to achieve a potential reproducibility of ± 1.09 mV for those electrodes where the metallic Ag concentration was increased through a photochemical reaction implemented by exposure to UV light [174]. The longer-term stability was only measured over 10 days, but in this time frame the potential only changed by ± 2 mV.

A reference electrode based on the electron conductor RuO_2 coated with a mixed layer of KCl and SiO_2, covered by a PVB membrane had E^0 repeatability of ± 0.5 mV, but when used with a pH electrode, the result was a slightly sub-Nernstian response and also a fairly high drift of 7 mV/h [175]. A 3D-printed non-plasticized PVC disk loaded with KCl and placed in contact with a Ag/AgCl wire was able to give a standard deviation in potentials of ± 0.01 V for a batch of 50 electrodes [176]. These reference electrodes were not tested extensively in terms of interference from various electrolytes, but the electrodes were reported to be stable over a 3 month period.

3.6.2 Ionic Liquid Reference Electrodes

Other methods to prepare solid-contact reference electrodes include electrodes with ionic liquid-doped reference membranes, where the distribution of an ionic liquid across the phase boundary between a reference membrane and the sample determines the reference potential. A comparison of reference electrodes containing ionic liquids and those containing trapped hydrophilic salts is illustrated in Figure 16. Reference electrodes with three-dimensionally ordered macroporous carbon as transducer that were coated with plasticized PVC membranes doped with an ionic liquid exhibited a very low drift in response of less than 0.1 mV/h over 15 days [177]. Interference from pH at low pH was shown to result from protonation of bis(trifluoromethylsulfonyl)imide, an issue evidently common with any other ionic liquid reference electrode using the same ionic liquid anion.

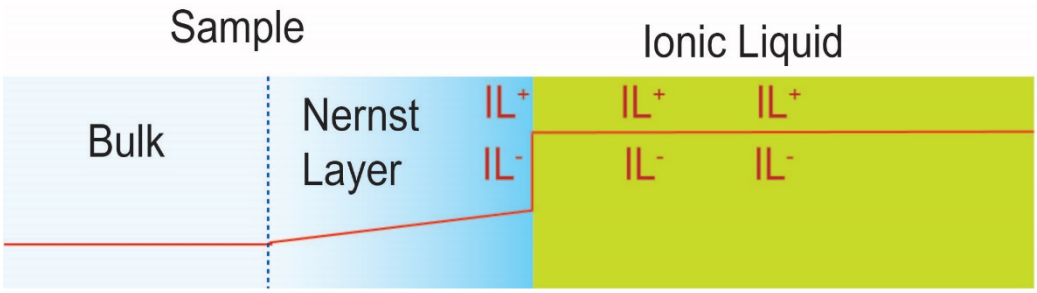

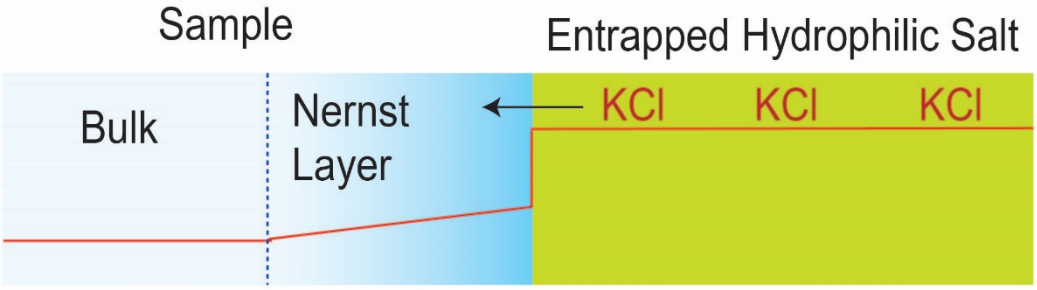

Figure 16: Relative concentrations of an ionic liquid (top) and trapped hydrophilic salt (bottom) in the sample bulk, Nernst diffusion layer, and membrane for membrane-based reference electrodes. These reference electrodes function through partitioning of the ionic liquid or trapped hydrophilic salt across the interface between the reference membrane and the sample, thereby determining the phase boundary potential. In particular in the case of hydrophilic salts, the reference membrane may be heterogeneous.

PVC plasticized with *o*-NPOE and doped with 1-methyl-3-octylimidazolium bis(trifluoromethylsulfonyl)imide applied over a carbon rod using a Co(II/III) tris(phenanthroline) redox buffer as transducer gave E^0 values with a standard deviation of ± 2.1 mV [180]. On a gold substrate modified with a 1-hexanethiol layer, the standard deviation was as

low as ± 1.5 mV, although the reference electrodes were determined to be stable for only about 24 h. A combination of CIM carbon and a cobalt (II/III) tris(dinonylbipyridine) redox buffer as the solid contact has also been investigated [181]. Here, the reproducibility of multiple reference electrodes measured versus an ISE showed E^0 values of ± 2.8 mV, with drift over a 110 hour period as low as 1.7 μV/h. These reference membranes were also used in disposable paper-based sensors. A biocompatible fluorosilicone matrix doped with 1-methyl-3-octylimidazolium bis(trifluoromethylsulfonyl)imide was used to fabricate reference membranes used in a solid-contact reference electrode using CIM carbon as the transducer [178]. These electrodes resulted in a drift of 112 μV/h over 5.8 days in a diluted animal serum solution and showed no potential change in the biologically relevant concentration ranges of blood electrolytes K^+, Na^+, Cl^-, HPO_4^{2-}, $H_2PO_4^-$, and H^+, although device-to-device potential reproducibility was not reported.

A polymerization-induced microphase separated membrane prepared using a copolymer of methyl methacrylate, styrene, and divinylbenzene has been used as an ionic liquid based reference membrane, with the bis-(trifluoromethyl sulfonyl)imide salts of 1-octyl-3-methylimidazolium or 1-dodecyl-3-methylimidazolium as ionic liquids. For the 12-carbon chain ionic liquid, the drift was 0.7 mV/h over 24 h, with a standard deviation of ± 2.0 mV [182]. Ionic liquid reference electrodes using a methacrylate-based membrane that was covalently attached to the underlying polymer substrate showed reproducibility of ± 10 mV, with a drift on average of 180 μV/h measured over a single day [43].

PEDOT polymerized from a solution in an ionic liquid and topped with a blend of butyl acrylate and *n*-decyl methacrylate doped with the ionic liquid has also been used for reference electrode construction [179]. The optimized reference electrodes were reproducible within a

standard deviation of 5 mV, although these electrodes exhibited some response to changing Na^+ and K^+ concentrations.

However, as has been recently discussed, the use of ionic liquid based reference electrodes can be problematic when the ISE is exposed to the ionic liquid that is continuously released from the reference electrode [184]. It was pointed out that one way to minimize these effects is to increase the sample size, which is not always possible. Another problem that ionic liquid reference electrodes share with reference electrodes comprising conventional salt bridges is the lifetime limitation, as the ionic liquid is continually leaching from the reference membrane and eventually will be exhausted. Lindner has presented extensive studies on the stability of ionic liquid reference electrodes prepared with different types of ionic liquids and under different sample flow rates [164]. Others have pointed out that the validation methods for ionic liquid reference electrodes are often not standardized, making comparison difficult [185]. To address the potential toxicity of ionic liquids, amino acid anions have been used as the anionic portion of ionic liquids for reference membranes [185].

3.6.3 Reference Electrodes with Pulsed Current Electrolyte Release

One approach to reference electrodes that overcomes the inherent lifetime limitation of many other reference electrodes is that of using current pulses to release controlled amounts of ions from a reference membrane to establish the reference potential. This was first demonstrated using plasticized PVC membranes containing tetrabutylammonium ions, which were released into the samples as the result of the application of current pulses in the range of a few microamperes [163]. The potentiometric measurement is performed immediately following the current pulse, resulting in a stable potential as the tetrabutylammonium has not yet diffused away from the membrane. More recently, this approach has been also applied to a solid-state Ag/AgI

device, which releases iodide on current application. Notably, the released iodide was recaptured by the electrode by application of a potential after the potentiometric measurement [186]. An advantage of the Ag/AgI implementation is the lower electrical resistance of the device as compared to the resistance of doped plasticized PVC membranes. Although these reference electrodes require more complex instrumentation capable of current application, they overcome lifetime limitations associated with miscible liquid junction and ionic liquid reference electrodes.

4. Conclusions

Among the various transduction systems described in this review, the most reliable ones to achieve E^0 reproducibilities of ± 1.0 mV or lower are those that use a redox buffer that defines the redox potential and includes two states of the buffer in approximately equal concentrations. Using conducting polymers alone as transducer, E^0 standard deviations on the order of ± 3.0 mV are often obtained, but few reports of reproducibilities lower than ± 1.0 mV exist. The use of prepolarization to set batches of electrodes to the same potential is also a promising method for improved reproducibility, although subsequent EMF drift needs to be considered carefully. There are fewer examples of low E^0 standard deviations with purely capacitive interfaces.

Long-term stability of the response is generally improved by the presence of a highly hydrophobic conducting polymers such as PEDOT or a derivative thereof but has also been observed with intercalation compounds. The drift of capacitive interfaces is lowest when using high surface area materials such as 3DOM, CIM carbon, and carbon black while CNTs as transducers provide somewhat larger EMF drifts. The best performing redox active transducers for which drift is reported exhibit drifts of similar magnitudes to the best performing capacitive transducers.

Hybrid materials have been investigated with the aim to gain advantages of both redox-active and capacitive interfaces, although there are few hybrid materials that have been shown to exhibit both outstanding E^0 reproducibilities and drift characteristics. Table 4 shows that to date most ISEs with a hybrid transducer material have E^0 reproducibilities or potential drifts that are not as low as for the better solid-contact ISEs with transducers that have only redox buffer or capacitive interfaces. For other hybrid transducer systems, either E^0 reproducibility or potential drift have not been reported. The most notable exception that appears to confirm the advantage of hybrid transducer systems are electrodes with CIM carbon transducers in the presence of a Co(III)/Co(II) redox buffer [60]. The other most promising hybrid transducer system combines poly(3-octylthiophene-2,5-diyl) with ruthenium dioxide nanoparticles [159].

Although it has become more common in recent years to report a standard deviation for E^0, some publications still do not report this metric, making it difficult to compare work without it to other systems. Long-term stability is even more difficult to compare between studies, as often the timeframe during which the drift was observed varies, and some studies focus more on retention of response slope, limit of detection, and selectivity as opposed to drift and absolute potential values. Other variability arises from the different exposure of ISEs and reference electrodes during long-term testing. To make it easier for researchers to compare different designs of solid-contact ISEs and reference electrodes and, thereby, facilitate progress in this field, we encourage investigators to consider the criteria for analyzing and reporting performance characteristics as summarized in Table 1.

Much effort has been put forth into the development of ISEs than can be used in a calibration-free manner. As this field progresses, a clear definition and explanation of what calibration-free means in the context of specific applications will help those from within and

outside the field to have a better understanding of the implications of such a description. Although there have been many improvements in terms of reproducibility and drift, there is still room to enhance the performance of solid-contact ISEs and reference electrodes in order to achieve the ultimate goal of mass-produced sensors that can be used without individual calibration and with little or no maintenance over time periods of weeks or months. Notably, sensors with a high E^0 reproducibility and low drift are also very robust sensors that will perform particularly well even when calibration-free operation is not a high priority.

Sensors with E^0 standard deviation lower than 1 mV have been developed, as have sensors that have adequate potential stability over the course of days or even weeks. Sensors will be viable for many applications if they combine these two characteristics and also possess reproducibility between batches in addition to within single batches. While desirable for other applications, lowering the standard deviation of E^0 and EMF drift to the next lower levels of 0.1 mV and 0.1 μV/h, respectively, is currently out of reach for anyone working in the field and will require continued systematic studies of all individual components and phase boundaries of solid-contact ISEs and reference electrodes.

Acknowledgments

This work was supported by the National Science Foundation (CHE-1710024) to P.B. as well as a Kenneth E. & Marion S. Owens Endowed Fellowship from the University of Minnesota, a ThinkSwiss fellowship from the Swiss State Secretariat for Education, Research and Innovation, and a Graduate Research Fellowship from the National Science Foundation to C.R.R.

References

[1] E. Bakker, Can calibration-free sensors be realized?, ACS Sens. 1 (2016) 838-841.
[2] M. Parrilla, M. Cuartero, G.A. Crespo, Wearable potentiometric ion sensors, TrAC, Trends Anal. Chem. 110 (2019) 303-320.
[3] G.A. Crespo, Recent advances in ion-selective membrane electrodes for in situ environmental water analysis, Electrochim. Acta 245 (2017) 1023-1034.
[4] J. Bobacka, A. Ivaska, A. Lewenstam, Potentiometric ion sensors based on conducting polymers, Electroanalysis 15 (2003) 366-374.
[5] A. Michalska, All-solid-state ion selective and all-solid-state reference electrodes, Electroanalysis 24 (2012) 1253-1265.
[6] R. De Marco, G. Clarke, B. Pejcic, Ion-selective electrode potentiometry in environmental analysis, Electroanalysis 19 (2007) 1987-2001.
[7] D. Ammann, W.E. Morf, P. Anker, P.C. Meier, E. Pretsch, W. Simon, Neutral carrier based ion-selective electrodes, Ion-Sel. Electrode Rev. 5 (1983) 3-92.
[8] E. Bakker, P. Bühlmann, E. Pretsch, Carrier-based ion-selective electrodes and bulk optodes. 1. General characteristics, Chem. Rev. 97 (1997) 3083-3132.
[9] P. Bühlmann, E. Pretsch, E. Bakker, Carrier-based ion-selective electrodes and bulk optodes. 2. Ionophores for potentiometric and optical sensors, Chem. Rev. 98 (1998) 1593-1687.
[10] P. Bühlmann, L.D. Chen, in: P.A. Gale and J.W. Steed (Eds.), Ion-selective electrodes with ionophore-doped sensing membranes John Wiley and Sons, Ltd. 2012.
[11] E. Zdrachek, E. Bakker, Potentiometric sensing, Anal. Chem. 91 (2019) 2-26.
[12] J.W. Ding, W. Qin, Recent advances in potentiometric biosensors, TrAC, Trends Anal. Chem. 124 (2020) 115803-115814.
[13] E. Hupa, U. Vanamo, J. Bobacka, Novel ion-to-electron transduction principle for solid-contact ISEs, Electroanalysis 27 (2015) 591-594.
[14] U. Vanamo, E. Hupa, V. Yrjana, J. Bobacka, New signal readout principle for solid-contact ion-selective electrodes, Anal. Chem. 88 (2016) 4369-4374.
[15] R.W. Cattrall, H. Freiser, Coated wire ion selective electrodes, Anal. Chem. 43 (1971) 1905-1906.
[16] J. Bobacka, T. Lindfors, M. McCarrick, A. Ivaska, A. Lewenstam, Single piece all-solid-state ion-selective electrode, Anal. Chem. 67 (1995) 3819-3823.
[17] M. Vazquez, J. Bobacka, A. Ivaska, Potentiometric sensors for Ag^+ based on poly(3-octylthiophene) (POT), J. Solid State Electrochem. 9 (2005) 865-873.
[18] M. Fibbioli, K. Bandyopadhyay, S.G. Liu, L. Echegoyen, O. Enger, F. Diederich, P. Bühlmann, E. Pretsch, Redox-active self-assembled monolayers as novel solid contacts for ion-selective electrodes, Chem. Commun. (2000) 339-340.
[19] B.P. Nikolskii, E.A. Materova, Solid contact in membrane ion-selective electrodes, Ion-Selective Electrode Reviews, 7 (1985) 3-39.
[20] A. Cadogan, Z.Q. Gao, A. Lewenstam, A. Ivaska, D. Diamond, All-solid-state sodium-selective electrode based on a calixarene ionophore in a poly(vinyl chloride) membrane with a polypyrrole solid contact, Anal. Chem. 64 (1992) 2496-2501.
[21] J. Hu, A. Stein, P. Bühlmann, Rational design of all-solid-state ion-selective electrodes and reference electrodes, TrAC, Trends Anal. Chem. 76 (2016) 102-114.
[22] E. Lindner, R.E. Gyurcsanyi, Quality control criteria for solid-contact, solvent polymeric membrane ion-selective electrodes, J. Solid State Electrochem. 13 (2009) 51-68.

[23] W.E. Morf, The principles of ion-selective electrodes and of membrane transport, Elsevier New York 1981.
[24] N. He, S. Papp, T. Lindfors, L. Hofler, R.M. Latonen, R.E. Gyurcsanyi, Pre-polarized hydrophobic conducting polymer solid-contact ion selective electrodes with improved potential reproducibility, Anal. Chem. 89 (2017) 2598-2605.
[25] E. Bakker, E. Pretsch, P. Bühlmann, Selectivity of potentiometric ion sensors, Anal. Chem. 72 (2000) 1127-1133.
[26] I. Yilmaz, L.D. Chen, X.V. Chen, E.L. Anderson, R.C. da Costa, J.A. Gladysz, P. Bühlmann, Potentiometric selectivities of lonophore-doped ion-selective membranes: Concurrent presence of primary ion or interfering ion complexes of multiple stoichiometries, Anal. Chem. 91 (2019) 2409-2417.
[27] S. Amemiya, P. Bühlmann, K. Odashima, A generalized model for apparently "non-nernstian" equilibrium responses of ionophore-based ion-selective electrodes. 1. Independent complexation of the ionophore with primary and secondary ions, Anal. Chem. 75 (2003) 3329-3339.
[28] Analytical Methods Committee, Is my calibration linear?, Analyst 119 (1994) 2363-2366.
[29] Laboratory regulations, Code of Federal Regulations, Section 493.931, Title 42, 2003.
[30] S. Papp, M. Bojtar, R.E. Gyurcsanyi, T. Lindfors, Potential reproducibility of potassium-selective electrodes having perfluorinated alkanoate side chain functionalized poly(3,4-ethylenedioxytiophene) as a hydrophobic solid contact, Anal. Chem. 91 (2019) 9111-9118.
[31] E. Jaworska, M. Mazur, K. Maksymiuk, A. Michalska, Fate of poly(3-octylthiophene) transducer in solid contact ion-selective electrodes, Anal. Chem. 90 (2018) 2625-2630.
[32] K.N. Mikhelson, A. Lewenstam, S.E. Didina, Contribution of the diffusion potential to the membrane potential and to the ion-selective electrode response, Electroanalysis 11 (1999) 793-798.
[33] M. Guzinski, J.M. Jarvis, B.D. Pendley, E. Lindner, Equilibration time of solid contact ion-selective electrodes, Anal. Chem. 87 (2015) 6654-6659.
[34] T. Forrest, E. Zdrachek, E. Bakker, Thin layer membrane systems as rapid development tool for potentiometric solid contact ion-selective electrodes, Electroanalysis 32 (2020) 799-804.
[35] V.V. Cosofret, M. Erdösy, E. Lindner, T.A. Johnson, R.P. Buck, W.J. Kao, M.R. Neuman, J.M. Anderson, Ion-selective microchemical sensors with reduced preconditioning time. Membrane biostability studies and applications in blood analysis, Anal. Lett. 27 (1994) 3039-3063.
[36] C.G. Zoski, Handbook of electrochemistry, Elsevier, 2007.
[37] Q.S. Ye, G. Horvai, A. Toth, I. Bertoti, M. Botreau, T.M. Duc, Studies of ion selective solvent polymeric membranes by x-ray photoelectron spectroscopy and time-of-flight static secondary ion mass spectroscopy, Anal. Chem. 70 (1998) 4241-4246.
[38] Q.S. Ye, S. Borbely, G. Horvai, Microstructure of ion selective plasticized PVC membranes studied by small angle neutron scattering, Anal. Chem. 71 (1999) 4313-4320.
[39] M. Kobashi, H. Takeuchi, Inhomogeneity of spin-coated and cast non-regioregular poly(3-hexylthiophene) films. Structures and electrical and photophysical properties, Macromolecules 31 (1998) 7273-7278.
[40] M. Vazquez, J. Bobacka, A. Ivaska, A. Lewenstam, Small-volume radial flow cell for all-solid-state ion-selective electrodes, Talanta 62 (2004) 57-63.

[41] M. Fibbioli, W.E. Morf, M. Badertscher, N.F. de Rooij, E. Pretsch, Potential drifts of solid-contacted ion-selective electrodes due to zero-current ion fluxes through the sensor membrane, Electroanalysis 12 (2000) 1286-1292.
[42] R. De Marco, J.-P. Veder, G. Clarke, A. Nelson, K. Prince, E. Pretsch, E. Bakker, Evidence of a water layer in solid-contact polymeric ion sensors, Phys. Chem. Chem. Phys. 10 (2008) 73-76.
[43] E.L. Anderson, S.A. Chopade, B. Spindler, A. Stein, T.P. Lodge, M.A. Hillmyer, P. Bühlmann, Solid-contact ion-selective and reference electrodes covalently attached to functionalized poly(ethylene terephthalate), Anal. Chem. 92 (2020) 7621-7629.
[44] M. Guzinski, J.M. Jarvis, P. D'Orazio, A. Izadyar, B.D. Pendley, E. Lindner, Solid-contact pH sensor without Co_2 interference with a superhydrophobic PEDOT-C-14 as solid contact: The ultimate "water layer" test, Anal. Chem. 89 (2017) 8468-8475.
[45] E.J. Fogt, D.F. Untereker, M.S. Norenberg, M.E. Meyerhoff, Response of ion-selective field-effect transistors to carbon-dioxide and organic-acids, Anal. Chem. 57 (1985) 1995-1998.
[46] M. Guzinski, J.M. Jarvis, F. Perez, B.D. Pendley, E. Lindner, R. De Marco, G.A. Crespo, R.G. Acres, R. Walker, J. Bishop, PEDOT (PSS) as solid contact for ion-selective electrodes: The influence of the PEDOT(PSS) film thickness on the equilibration times, Anal. Chem. 89 (2017) 3508-3516.
[47] J.-P. Veder, R. De Marco, G. Clarke, R. Chester, A. Nelson, K. Prince, E. Pretsch, E. Bakker, Elimination of undesirable water layers in solid-contact polymeric ion-selective electrodes, Anal. Chem. 80 (2008) 6731-6740.
[48] B. Paczosa-Bator, R. Piech, L. Cabaj, The influence of an intermediate layer on the composition stability of a polymeric ion-selective membrane, Electrochim. Acta 85 (2012) 104-109.
[49] T. Lindfors, Light sensitivity and potential stability of electrically conducting polymers commonly used in solid contact ion-selective electrodes, J. Solid State Electrochem. 13 (2009) 77-89.
[50] C. EspadasTorre, V. Oklejas, K. Mowery, M.E. Meyerhoff, Thromboresistant chemical sensors using combined nitric oxide release ion sensing polymeric films, J. Am. Chem. Soc. 119 (1997) 2321-2322.
[51] H.P. Zhang, G.M. Annich, J. Miskulin, K. Osterholzer, S.I. Merz, R.H. Bartlett, M.E. Meyerhoff, Nitric oxide releasing silicone rubbers with improved blood compatibility: Preparation, characterization, and in vivo evaluation, Biomaterials 23 (2002) 1485-1494.
[52] X.J. Jiang, P. Wang, R.N. Liang, W. Qin, Improving the biocompatibility of polymeric membrane potentiometric ion sensors by using a mussel-inspired polydopamine coating, 91 (2019) 6424-6429.
[53] N.K. Joon, N. He, T. Ruzgas, J. Bobacka, G. Lisak, PVC-based ion-selective electrodes with a silicone rubber outer coating with improved analytical performance, 91 (2019) 10524-10531.
[54] X.V. Chen, M.P.S. Mousavi, P. Bühlmann, Fluorous-phase ion-selective pH electrodes: Electrode body and ionophore optimization for measurements in the physiological ph range, 5 (2020) 13621-13629.
[55] T.J. Jiang, L.B. Qi, C. Hou, S.T. Fang, W. Qin, Self-sterilizing polymeric membrane sensors based on 6-chloroindole release for prevention of marine biofouling, 92 (2020) 12132-12136.

[56] L.B. Qi, T.J. Jiang, R.N. Liang, W. Qin, Polymeric membrane ion-selective electrodes with anti-biofouling properties by surface modification of silver nanoparticles, 328 (2021).
[57] Y.Z. Shao, Y.B. Ying, J.F. Ping, Recent advances in solid-contact ion-selective electrodes: Functional materials, transduction mechanisms, and development trends, Chem. Soc. Rev. 49 (2020) 4405-4465.
[58] J. Bobacka, A. Ivaska, A. Lewenstam, Potentiometric ion sensors, Chem. Rev. 108 (2008) 329-351.
[59] E.L. Anderson, P. Bühlmann, Electrochemical impedance spectroscopy of ion-selective membranes: Artifacts in two-, three-, and four-electrode measurements, Anal. Chem. 88 (2016) 9738-9745.
[60] J. Hu, X.U. Zou, A. Stein, P. Bühlmann, Ion-selective electrodes with colloid-imprinted mesoporous carbon as solid contact, Anal. Chem. 86 (2014) 7111-7118.
[61] V.F. Lvovich, Impedance spectroscopy: Applications to electrochemical and dielectric phenomena, John Wiley & Sons, Inc., 2012.
[62] B.T. Mark E. Orazem, Electrochemical impedance spectroscopy John Wiley & Sons, Inc., 2008.
[63] T.M. Nahir, R.P. Buck, Steady-state-current impedance spectroscopy of plasticized pvc membranes containing neutral ion carriers, Electrochim, Acta 38 (1993) 2691-2697.
[64] K. Toth, E. Graf, G. Horvai, E. Pungor, R.P. Buck, Plasticized polyvinyl-chloride) properties and characteristics of valinomycin electrodes .2. Low-frequency, surface-rate, and warburg impedance characteristics, Anal. Chem. 58 (1986) 2741-2744.
[65] R.P. Buck, Impedances of membrane systems with metal and or ionic contacts, Electrochim. Acta 35 (1990) 1609-1617.
[66] M.A. Fierke, C.-Z. Lai, P. Bühlmann, A. Stein, Effects of architecture and surface chemistry of three-dimensionally ordered macroporous carbon solid contacts on performance of ion-selective electrodes, 82 (2010) 680-688.
[67] J. Bobacka, A. Ivaska, A. Lewenstam, Plasticizer-free all-solid-state potassium-selective electrode based on poly(3-octylthiophene) and valinomycin, 385 (1999) 195-202.
[68] T. Lindfors, J. Bobacka, A. Lewenstam, A. Ivaska, Impedance spectroscopic study on single-piece all-solid-state calcium-selective electrode based on polyaniline, Analyst 121 (1996) 1823-1827.
[69] J. Bobacka, Potential stability of all-solid-state ion-selective electrodes using conducting polymers as ion-to-electron transducers, Anal. Chem. 71 (1999) 4932-4937.
[70] A. Bard, Electrochemical methods: Fundamentals and applications, 2 Ed., John Wiley and Sons, Inc., 2000.
[71] J.P. Veder, R. De Marco, K. Patel, P.C. Si, E. Grygolowicz-Pawlak, M. James, M.T. Alam, M. Sohail, J. Lee, E. Pretsch, E. Bakker, Evidence for a surface confined ion-to-electron transduction reaction in solid-contact ion-selective electrodes based on poly(3-octylthiophene), Anal. Chem. 85 (2013) 10495-10502.
[72] M. Cuartero, J. Bishop, R. Walker, R.G. Acres, E. Bakker, R. De Marco, G.A. Crespo, Evidence of double layer/capacitive charging in carbon nanomaterial-based solid contact polymeric ion-selective electrodes, Chem. Commun. 52 (2016) 9703-9706.
[73] A. Hulanicki, M. Trojanowicz, Calcium-selective electrodes with PVC membranes and solid internal contacts, Anal. Chim. Acta 87 (1976) 411-417.

[74] D. Liu, R.K. Meruva, R.B. Brown, M.E. Meyerhoff, Enhancing emf stability of solid-state ion-selective sensors by incorporating lipophilic silver-ligand complexes within polymeric films, Anal. Chim. Acta 321 (1996) 173-183.
[75] J. Bobacka, M. McCarrick, A. Lewenstam, A. Ivaska, All-solid-state poly(vinyl chloride) membrane ion-selective electrodes with poly(3-octylthiophene) solid internal contact, Analyst 119 (1994) 1985-1991.
[76] J.M. Jarvis, M. Guzinski, B.D. Pendley, E. Lindner, Poly(3-octylthiophene) as solid contact for ion-selective electrodes: Contradictions and possibilities, J. Solid State Electrochem. 20 (2016) 3033-3041.
[77] J. Sutter, E. Lindner, R.E. Gyurcsanyi, E. Pretsch, A polypyrrole-based solid-contact Pb^{2+}-selective pvc-membrane electrode with a nanomolar detection limit, Anal. Bioanal. Chem. 380 (2004) 7-14.
[78] P. Pu, M. Zhang, Y.H. Li, L.N. Zhang, H.Y. Ren, P. Kong, L.P. Pan, Preparation and evaluation of a stable solid state ion selective electrode of polypyrrole/electrochemically reduced graphene/glassy carbon substrate for soil nitrate sensing, Int. J. Electrochem. Sci. 11 (2016) 4779-4793.
[79] M.K. Abd El-Rahman, M.R. Rezk, A.M. Mahmoud, M.R. Elghobashy, Design of a stable solid-contact ion-selective electrode based on polyaniline nanoparticles as ion-to-electron transducer for application in process analytical technology as a real-time analyzer, Sens. Actuators, B 208 (2015) 14-21.
[80] A.M. Mahmoud, M.K. Abd El-Rahman, M.R. Elghobashy, M.R. Rezk, Carbon nanotubes versus polyaniline nanoparticles; which transducer offers more opportunities for designing a stable solid contact ion-selective electrode, J. Electroanal. Chem. 755 (2015) 122-126.
[81] N. Abramova, J. Moral-Vico, J. Soley, C. Ocana, A. Bratov, Solid contact ion sensor with conducting polymer layer copolymerized with the ion-selective membrane for determination of calcium in blood serum, Anal. Chim. Acta 943 (2016) 50-57.
[82] M. Piek, R. Piech, B. Paczosa-Bator, TTF-TCNQ solid contact layer in all-solid-state ion-selective electrodes for potassium or nitrate determination, J. Electrochem. Soc. 165 (2018) B60-B65.
[83] P.C. Hauser, D.W.L. Chiang, G.A. Wright, A potassium-ion selective electrode with valinomycin based poly(vinyl chloride) membrane and a poly(vinyl ferrocene) solid contact, Anal. Chim. Acta 302 (1995) 241-248.
[84] E. Grygolowicz-Pawlak, K. Wygladacz, S. Sek, R. Bilewicz, Z. Brzozka, E. Malinowska, Studies on ferrocene organothiol monolayer as an intermediate phase of potentiometric sensors with gold inner contact, Sens. Actuators, B 111 (2005) 310-316.
[85] X.U. Zou, J.H. Cheong, B.J. Taitt, P. Bühlmann, Solid contact ion-selective electrodes with a well-controlled Co(II)/Co(IIi) redox buffer layer, Anal. Chem. 85 (2013) 9350-9355.
[86] X.U. Zou, X.V. Zhen, J.H. Cheong, P. Bühlmann, Calibration-free ionophore-based ion-selective electrodes with a Co(II)/Co(III) redox couple-based solid contact, Anal. Chem. 86 (2014) 8687-8692.
[87] E. Jaworska, M.L. Naitana, E. Stelmach, G. Pomarico, M. Wojciechowski, E. Bulska, K. Maksymiuk, R. Paolesse, A. Michalska, Introducing cobalt(II) porphyrin/cobalt(III) corrole containing transducers for improved potential reproducibility and performance of all-solid-state ion-selective electrodes, Anal. Chem. 89 (2017) 7107-7114.

[88] Y.H. Cheong, L.Y. Ge, N.H. Zhao, L.K. Teh, G. Lisak, Ion selective electrodes utilizing a ferrocyanide doped redox active screen-printed solid contact - impact of electrode response to conditioning, J. Electroanal. Chem. 870 (2020) 114262-114268.
[89] M. Zhou, S. Gan, B. Cai, F. Li, W. Ma, D. Han, L. Niu, Effective solid contact for ion-selective electrodes: Tetrakis(4-chlorophenyl)borate (TB^-) anions doped nanocluster films, Anal. Chem. 84 (2012) 3480-3483.
[90] Q.B. An, L.S. Jiao, F. Jia, J.J. Ye, F.H. Li, S.Y. Gan, Q.X. Zhang, A. Ivaska, L. Niu, Robust single-piece all-solid-state potassium-selective electrode with monolayer-protected Au clusters, J. Electroanal. Chem. 781 (2016) 272-277.
[91] C. Wardak, Solid contact nitrate ion-selective electrode based on ionic liquid with stable and reproducible potential, Electroanalysis 26 (2014) 864-872.
[92] B. Bartoszewicz, S. Dabrowska, A. Lewenstam, J. Migdalski, Calibration free solid contact electrodes with two PVC based membranes, Sens. Actuators, B 274 (2018) 268-273.
[93] Y. Ishige, S. Klink, W. Schuhmann, Intercalation compounds as inner reference electrodes for reproducible and robust solid-contact ion-selective electrodes, Angew. Chem., Int. Ed. 55 (2016) 4831-4835.
[94] S. Klink, Y. Ishige, W. Schuhmann, Prussian blue analogues: A versatile framework for solid-contact ion-selective electrodes with tunable potentials, ChemElectrocChem 4 (2017) 490-494.
[95] J. Bobacka, Conducting polymer-based solid-state ion-selective electrodes, Electroanalysis 18 (2006) 7-18.
[96] J.F. Rubinson, Y.P. Kayinamura, Charge transport in conducting polymers: Insights from impedance spectroscopy, Chem. Soc. Rev. 38 (2009) 3339-3347.
[97] J. Maier, Physical chemistry of ionic materials: Ions and electrons in solids, John Wiley and Sons, Ltd. , West Sussex, England, 2004.
[98] Z. Plawinska, A. Michalska, K. Maksymiuk, Optimization of capacitance of conducting polymer solid contact in ion-selective electrodes, Electrochim. Acta 187 (2016) 397-405.
[99] M.B. Garada, B. Kabagambe, Y. Kim, S. Amemiya, Ion-transfer voltammetry of perfluoroalkanesulfonates and perfluoroalkanecarboxylates: Picomolar detection limit and high lipophilicity, Anal. Chem. 86 (2014) 11230-11237.
[100] J. Sutter, A. Radu, S. Peper, E. Bakker, E. Pretsch, Solid-contact polymeric membrane electrodes with detection limits in the subnanomolar range, 523 (2004) 53-59.
[101] P. Sjoberg-Eerola, J. Nylund, J. Bobacka, A. Lewenstam, A. Ivaska, Soluble semiconducting poly(3-octylthiophene) as a solid-contact material in all-solid-state chloride sensors, 134 (2008) 878-886.
[102] D. Kaluza, E. Jaworska, M. Mazur, K. Maksymiuk, A. Michalska, Multiwalled carbon nanotubes-poly(3-octylthiophene-2,5-diyl) nanocomposite transducer for ion-selective electrodes: Raman spectroscopy insight into the transducer/membrane interface, Anal. Chem. 91 (2019) 9010-9017.
[103] T. Lindfors, H. Aarnio, A. Ivaska, Potassium-selective electrodes with stable and geometrically well-defined internal solid contact based on nanoparticles of polyaniline and plasticized poly(vinyl chloride), Anal. Chem. 79 (2007) 8571-8577.
[104] T. Lindfors, J. Szuecs, F. Sundfors, R.E. Gyurcsanyi, Polyaniline nanoparticle-based solid-contact silicone rubber ion-selective electrodes for ultratrace measurements, Anal. Chem. 82 (2010) 9425-9432.

[105] C.C. Liu, X.H. Jiang, Y.Y. Zhao, W.W. Jiang, Z.M. Zhang, L.M. Yu, A solid-contact Pb^{2+}- selective electrode based on electrospun polyaniline microfibers film as ion-to-electron transducer, Electrochim. Acta 231 (2017) 53-60.
[106] T. Lindfors, A. Ivaska, Stability of the inner polyaniline solid contact layer in all-solid-state K^{+}-selective electrodes based on plasticized poly(vinyl chloride), Anal. Chem. 76 (2004) 4387-4394.
[107] U. Vanamo, J. Bobacka, Electrochemical control of the standard potential of solid-contact ion-selective electrodes having a conducting polymer as ion-to-electron transducer, Electrochim. Acta 122 (2014) 316-321.
[108] U. Vanamo, J. Bobacka, Instrument-free control of the standard potential of potentiometric solid-contact ion-selective electrodes by short-circuiting with a conventional reference electrode, Anal. Chem. 86 (2014) 10540-10545.
[109] D. Lakshmi, M.J. Whitcombe, F. Davis, I. Chianella, E.V. Piletska, A. Guerreiro, S. Subrahmanyam, P.S. Brito, S.A. Fowler, S.A. Piletsky, Chimeric polymers formed from a monomer capable of free radical, oxidative and electrochemical polymerisation, Chem. Commun. (2009) 2759-2761.
[110] N. He, R.E. Gyurcsanyi, T. Lindfors, Electropolymerized hydrophobic polyazulene as solid-contacts in potassium-selective electrodes, Analyst 141 (2016) 2990-2997.
[111] M. Pawlak, E. Grygolowicz-Pawlak, E. Bakker, Ferrocene bound poly(vinyl chloride) as ion to electron transducer in electrochemical ion sensors, Anal. Chem. 82 (2010) 6887-6894.
[112] J.P. Hurvois, C. Moinet, Reactivity of ferrocenium cations with molecular oxygen in polar organic solvents: Decomposition, redox reactions and stabilization, J. Organomet. Chem. 690 (2005) 1829-1839.
[113] P.J. Peerce, A.J. Bard, Polymer-films on electrodes. 2. Film structure and mechanism of electron-transfer with electrodeposited poly(vinylferrocene), J. Electroanal. Chem. 112 (1980) 97-115.
[114] S. Timpanaro, M. Kemerink, F.J. Touwslager, M.M. De Kok, S. Schrader, Morphology and conductivity of PEDOT/PSS films studied by scanning-tunneling microscopy, Chem. Phys. Lett. 394 (2004) 339-343.
[115] J. Stejskal, D. Hlavata, P. Holler, M. Trchova, J. Prokes, I. Sapurina, Polyaniline prepared in the presence of various acids: A conductivity study, Polymer International 53 (2004) 294-300.
[116] M. Fibbioli, K. Bandyopadhyay, S.G. Liu, L. Echegoyen, O. Enger, F. Diederich, D. Gingery, P. Bühlmann, H. Persson, U.W. Suter, E. Pretsch, Redox-active self-assembled monolayers for solid-contact polymeric membrane ion-selective electrodes, Chem. Mater. 14 (2002) 1721-1729.
[117] E. Grygolowicz-Pawlak, K. Plachecka, Z. Brzozka, E. Malinowska, Further studies on the role of redox-active monolayer as intermediate phase of solid-state sensors, Sens. Actuators, B 123 (2007) 480-487.
[118] F. Scholz, H. Kahlert, U. Hasse, A. Albrecht, A.C.T. Kuate, K. Jurkschat, A solid-state redox buffer as interface of solid-contact ISEs, Electrochem. Commun. 12 (2010) 955-957.
[119] E. Lindner, V.V. Cosofret, S. Ufer, R.P. Buck, R.P. Kusy, R.B. Ash, H.T. Nagle, Flexible (Kapton-based) microsensor arrays of high-stability for cardiovascular applications, J. Chem. Soc.-Faraday Trans. 89 (1993) 361-367.

[120] X.V. Zhen, C.R. Rousseau, P. Bühlmann, Redox buffer capacity of ion-selective electrode solid contacts doped with organometallic complexes, Anal. Chem. 90 (2018) 11000-11007.
[121] X.U. Zou, B. J. Taitt, P. Bühlmann, Unpublished results.
[122] L.F.J. Durselen, U. Oesterle, S. Schuppisser, H.V. Pham, Y. Miyahara, W.E. Morf, W. Simon, New solid-state contact for ion-selective liquid membrane electrodes, Chimia 44 (1990) 214-215.
[123] M. Fujiwara, Direct observation of ion behavior in a membrane containing valinomycin, J. Electroanal. Chem. 296 (1990) 259-262.
[124] M. Fujiwara, Analysis of ion behavior and potentials in a Na^+ ion-selective membrane containing methyl monensin, Clin. Chem. 37 (1991) 1375-1378.
[125] M.L. Honig, C.R. Rousseau, P. Bühlmann, Hydrophilic redox buffers in ion-selective electrodes. PittCon, Chicago, IL, USA, 2020.
[126] K. Pietrzak, C. Wardak, R. Lyszczek, Solid contact nitrate ion-selective electrode based on cobalt(II) complex with 4,7-diphenyl-1,10-phenanthroline, Electroanalysis 32 (2020) 724-731.
[127] S. Komaba, T. Akatsuka, K. Ohura, C. Suzuki, N. Yabuuchi, S. Kanazawa, K. Tsuchiya, T. Hasegawa, All-solid-state ion-selective electrodes with redox-active lithium, sodium, and potassium insertion materials as the inner solid-contact layer, Analyst 142 (2017) 3857-3866.
[128] C.-Z. Lai, M.A. Fierke, A. Stein, P. Bühlmann, Ion-selective electrodes with three-dimensionally ordered macroporous carbon as the solid contact, Anal. Chem. 79 (2007) 4621-4626.
[129] T. Fayose, L. Mendecki, S. Ullah, A. Radu, Single strip solid contact ion selective electrodes on a pencil-drawn electrode substrate, Anal. Methods 9 (2017) 1213-1220.
[130] Z.D.Y. Jiang, X. Xi, S. Qiu, D.Q. Wu, W. Tang, X.J. Guo, Y.Z. Su, R.L. Liu, Ordered mesoporous carbon sphere-based solid-contact ion-selective electrodes, J. Mater. Sci. 54 (2019) 13674-13684.
[131] E.J. Parra, G.A. Crespo, J. Riu, A. Ruiz, F.X. Rius, Ion-selective electrodes using multi-walled carbon nanotubes as ion-to-electron transducers for the detection of perchlorate, Analyst 134 (2009) 1905-1910.
[132] F.X. Rius-Ruiz, G.A. Crespo, D. Bejarano-Nosas, P. Blondeau, J. Riu, F.X. Rius, Potentiometric strip cell based on carbon nanotubes as transducer layer: Toward low-cost decentralized measurements, Anal. Chem. 83 (2011) 8810-8815.
[133] T. Zhang, Y.Q. Chai, R. Yuan, J.X. Guo, Nanostructured multi-walled carbon nanotubes derivate based on carbon paste electrode for potentiometric detection of Ag^+ ions, Anal. Methods 4 (2012) 454-459.
[134] S. Papp, J. Kozma, T. Lindfors, R.E. Gyurcsanyi, Lipophilic multi-walled carbon nanotube-based solid contact potassium ion-selective electrodes with reproducible standard potentials. A comparative study, Electroanalysis 32 (2020) 867-873.
[135] M. Parrilla, J. Ferre, T. Guinovart, F.J. Andrade, Wearable potentiometric sensors based on commercial carbon fibres for monitoring sodium in sweat, Electroanalysis 28 (2016) 1267-1275.
[136] R. Hernandez, J. Riu, J. Bobacka, C. Valles, P. Jimenez, A.M. Benito, W.K. Maser, F. Xavier Rius, Reduced graphene oxide films as solid transducers in potentiometric all-solid-state ion-selective electrodes, J. Phys. Chem. C 116 (2012) 22570-22578.

[137] E. Jaworska, W. Lewandowski, J. Mieczkowski, K. Maksymiuk, A. Michalska, Critical assessment of graphene as ion-to-electron transducer for all-solid-state potentiometric sensors, Talanta 97 (2012) 414-419.
[138] T.J. Yin, J.H. Li, W. Qin, An all-solid-state polymeric membrane Ca^{2+}-selective electrode based on hydrophobic alkyl-chain-functionalized graphene oxide, Electroanalysis 29 (2017) 821-827.
[139] B. Paczosa-Bator, All-solid-state selective electrodes using carbon black, Talanta 93 (2012) 424-427.
[140] B. Paczosa-Bator, L. Cabaj, R. Piech, K. Skupien, Potentiometric sensors with carbon black supporting platinum nanoparticles, Anal. Chem. 85 (2013) 10255-10261.
[141] H.J. Park, J.M. Jeong, J.H. Yoon, S.G. Son, Y.K. Kim, D. Kim, K.G. Lee, B.G. Choi, Preparation of ultrathin defect-free graphene sheets from graphite via fluidic delamination for solid-contact ion-to-electron transducers in potentiometric sensors, J. Colloid Interface Sci. 560 (2020) 817-824.
[142] B. Paczosa-Bator, Ion-selective electrodes with superhydrophobic polymer/carbon nanocomposites as solid contact, Carbon 95 (2015) 879-887.
[143] M.P.S. Mousavi, A. Ainla, E.K.W. Tan, M.K. Abd El-Rahman, Y. Yoshida, L. Yuan, H.H. Sigurslid, N. Arkan, M.C. Yip, C.K. Abrahamsson, S. Homer-Vanniasinkam, G.M. Whitesides, Ion sensing with thread-based potentiometric electrodes, Lab Chip 18 (2018) 2279-2290.
[144] E. Jaworska, M. Wojcik, A. Kisiel, J. Mieczkowski, A. Michalska, Gold nanoparticles solid contact for ion-selective electrodes of highly stable potential readings, Talanta 85 (2011) 1986-1989.
[145] Y.L. Liu, Y. Liu, R. Yan, Y.Y. Gao, P. Wang, Bimetallic AuCu nanoparticles coupled with multi-walled carbon nanotubes as ion-to-electron transducers in solid-contact potentiometric sensors, Electrochim. Acta 331 (2020).
[146] B. Paczosa-Bator, L. Cabaj, R. Piech, K. Skupien, Platinum nanoparticles intermediate layer in solid-state selective electrodes, Analyst 137 (2012) 5272-5277.
[147] T.J. Yin, D.W. Pan, W. Qin, All-solid-state polymeric membrane ion-selective miniaturized electrodes based on a nanoporous gold film as solid contact, Anal. Chem. 86 (2014) 11038-11044.
[148] G.A. Crespo, S. Macho, F. Xavier Rius, Ion-selective electrodes using carbon nanotubes as ion-to-electron transducers, Anal. Chem. 80 (2008) 1316-1322.
[149] C.L. Yang, Y.Q. Chai, R. Yuan, J.X. Guo, F. Jia, Ligand-modified multi-walled carbon nanotubes for potentiometric detection of silver, Anal. Sci. 28 (2012) 275-282.
[150] D.J. Yuan, A.H.C. Anthis, M.G. Afshar, N. Pankratova, M. Cuartero, G.A. Crespo, E. Bakker, All-solid-state potentiometric sensors with a multiwalled carbon nanotube inner transducing layer for anion detection in environmental samples, Anal. Chem. 87 (2015) 8640-8645.
[151] G. Matzeu, C. Zuliani, D. Diamond, Solid-contact ion-selective electrodes (ISEs) based on ligand functionalised gold nanoparticles, Electrochim. Acta 159 (2015) 158-165.
[152] N.M. Ivanova, I.V. Podeshvo, M.Y. Goikhman, A.V. Yakimanskii, K.N. Mikhelson, Potassium-selective solid contact electrodes with poly(amidoacid) Cu(I) complex, electron-ion exchanging resin and different sorts of carbon black in the transducer layer, Sens. Actuators, B 186 (2013) 589-596.

[153] Q.Q. Sun, W.Z. Li, B. Su, Highly hydrophobic solid contact based on graphene-hybrid nanocomposites for all solid state potentiometric sensors with well-formulated phase boundary potentials, J. Electroanal. Chem. 740 (2015) 21-27.
[154] Z.A. Boeva, T. Lindfors, Few-layer graphene and polyaniline composite as ion-to-electron transducer in silicone rubber solid-contact ion-selective electrodes, Sens. Actuators, B 224 (2016) 624-631.
[155] J. Szucs, T. Lindfors, J. Bobacka, R.E. Gyurcsanyi, Ion-selective electrodes with 3D nanostructured conducting polymer solid contact, Electroanalysis 28 (2016) 778-786.
[156] J.H. Li, T.J. Yin, W. Qin, An effective solid contact for an all-solid-state polymeric membrane Cd^{2+}-selective electrode: Three-dimensional porous graphene-mesoporous platinum nanoparticle composite, Sens. Actuators, B 239 (2017) 438-446.
[157] M.A. Ali, X.R. Wang, Y.C. Chen, Y.Y. Jiao, N.K. Mahal, S. Moru, M.J. Castellano, J.C. Schnable, P.S. Schnable, L. Dong, Continuous monitoring of soil nitrate using a miniature sensor with poly(3-octyl-thiophene) and molybdenum disulfide nanocomposite, ACS Appl. Mater. Interfaces 11 (2019) 29195-29206.
[158] J.N. Xu, F.H. Li, C. Tian, Z.Q. Song, Q.B. An, J.Y. Wang, D.X. Han, L. Niu, Tubular Au-TTF solid contact layer synthesized in a microfluidic device improving electrochemical behaviors of paper-based potassium potentiometric sensors, Electrochim. Acta 322 (2019).
[159] N. Lenar, B. Paczosa-Bator, R. Piech, Ruthenium dioxide nanoparticles as a high-capacity transducer in solid-contact polymer membrane-based pH-selective electrodes, Microchim. Acta 186 (2019).
[160] N. Lenar, B. Paczosa-Bator, R. Piech, Ruthenium dioxide as high-capacitance solid-contact layer in K^+-selective electrodes based on polymer membrane, J. Electrochem. Soc. 166 (2019) B1470-B1476.
[161] N. Lenar, B. Paczosa-Bator, R. Piech, A. Krolicka, Poly(3-octylthiophene-2,5-diyl) - nanosized ruthenium dioxide composite material as solid-contact layer in polymer membrane-based K^+-selective electrodes, Electrochim. Acta 322 (2019).
[162] L. Mendecki, K.A. Mirica, Conductive metal-organic frameworks as ion-to-electron transducers in potentiometric sensors, ACS Appl. Mater. Interfaces 10 (2018) 19248-19257.
[163] X.U. Zou, P. Bühlmann, Current pulse based reference electrodes without liquid junctions, 85 (2013) 3817-3821.
[164] E. Lindner, M. Guzinski, T.A. Khan, B.D. Pendley, Reference electrodes with ionic liquid salt bridge: When will these innovative novel reference electrodes gain broad acceptance?, ACS Sens. 4 (2019) 549-561.
[165] J.P. Wilburn, M. Ciobanu, N.I. Buss, D.R. Franceschetti, D.A. Lowy, Miniaturized reference electrodes with stainless steel internal reference elements, Anal. Chim. Acta 511 (2004) 83-89.
[166] A. Kisiel, H. Marcisz, A. Michalska, K. Maksymiuk, All-solid-state reference electrodes based on conducting polymers, Analyst 130 (2005) 1655-1662.
[167] S. Anastasova-Ivanova, U. Mattinen, A. Radu, J. Bobacka, A. Lewenstam, J. Migdalski, M. Danielewskic, D. Diamond, Development of miniature all-solid-state potentiometric sensing system, Sens. Actuators, B 146 (2010) 199-205.
[168] A. Kisiel, A. Michalska, K. Maksymiuk, E.A.H. Hall, All-solid-state reference electrodes with poly(*n*-butyl acrylate) based membranes, Electroanalysis 20 (2008) 318-323.

[169] A. Kisiel, M. Donten, J. Mieczkowski, F.X. Rius-Ruiz, K. Maksymiuk, A. Michalska, Polyacrylate microspheres composite for all-solid-state reference electrodes, Analyst 135 (2010) 2420-2425.
[170] F.X. Rius-Ruiz, D. Bejarano-Nosas, P. Blondeau, J. Riu, F.X. Rius, Disposable planar reference electrode based on carbon nanotubes and polyacrylate membrane, Anal. Chem. 83 (2011) 5783-5788.
[171] A. Kisiel, K. Kijewska, M. Mazur, K. Maksymiuk, A. Michalska, Polypyrrole microcapsules in all-solid-state reference electrodes, Electroanalysis 24 (2012) 165-172.
[172] K. Granholm, Z. Mousavi, T. Sokalski, A. Lewenstam, Analytical quality solid-state composite reference electrode manufactured by injection moulding, J. Solid State Electrochem. 18 (2014) 607-612.
[173] T. Guinovart, G.A. Crespo, F.X. Rius, F.J. Andrade, A reference electrode based on polyvinyl butyral (PVB) polymer for decentralized chemical measurements, Anal. Chim. Acta 821 (2014) 72-80.
[174] A. Lewenstam, T. Blaz, J. Migdalski, All-solid-state reference electrode with heterogeneous membrane, Anal. Chem. 89 (2017) 1068-1072.
[175] W. Lonsdale, M. Wajrak, K. Alameh, RuO_2 pH sensor with super-glue-inspired reference electrode, Sensors 17 (2017).
[176] A. Lewenstam, B. Bartoszewicz, J. Migdalski, A. Kochan, Solid contact reference electrode with a PVC-based composite electroactive element fabricated by 3D printing, Electrochem. Commun. 109 (2019) 106613-106616.
[177] T.T. Zhang, C.Z. Lai, M.A. Fierke, A. Stein, P. Bühlmann, Advantages and limitations of reference electrodes with an ionic liquid junction and three-dimensionally ordered macroporous carbon as solid contact, Anal. Chem. 84 (2012) 7771-7778.
[178] X.V. Chen, A. Stein, P. Bühlmann, Reference electrodes based on ionic liquid-doped reference membranes with biocompatible silicone matrixes, 5 (2020) 1717-1725.
[179] C. Zuliani, G. Matzeu, D. Diamond, A liquid-junction-free reference electrode based on a pedot solid-contact and ionogel capping membrane, Talanta 125 (2014) 58-64.
[180] X.U. Zou, L.D. Chen, C.Z. Lai, P. Bühlmann, Ionic liquid reference electrodes with a well-controlled Co(II)/Co(III) redox buffer as solid contact, Electroanalysis 27 (2015) 602-608.
[181] J.B. Hu, K.T. Ho, X.U. Zou, W.H. Smyrl, A. Stein, P. Bühlmann, All-solid-state reference electrodes based on colloid-imprinted mesoporous carbon and their application in disposable paper-based potentiometric sensing devices, Anal. Chem. 87 (2015) 2981-2987.
[182] S.A. Chopade, E.L. Anderson, P.W. Schmidt, T.P. Lodge, M.A. Hillmyer, P. Bühlmann, Self-supporting, hydrophobic, ionic liquid-based reference electrodes prepared by polymerization-induced microphase separation, ACS Sens. 2 (2017) 1498-1504.
[183] P. Lingenfelter, B. Bartoszewicz, J. Migdalski, T. Sokalski, M.M. Bucko, R. Filipek, A. Lewenstam, Reference electrodes with polymer-based membranes-comprehensive performance characteristics, Membranes 9 (2019).
[184] M.P.S. Mousavi, M.K. Abd El-Rahman, E.K.W. Tan, H.H. Sigurslid, N. Arkan, J.S. Lane, G.M. Whitesides, P. Bühlmann, Ionic liquid-based reference electrodes for miniaturized ion sensors: What can go wrong?, Sens. Actuator B-Chem. 301 (2019) 8.
[185] T.M. Galiullin, N.V. Pokhvishcheva, A.V. Kalinichev, M.A. Peshkova, Evaluation of ionic liquids based on amino acid anions for use in liquid-junction free reference electrodes, Electroanalysis 31 (2019) 1708-1718.

[186] W.Y. Gao, E. Zdrachek, X.J. Xie, E. Bakker, A solid-state reference electrode based on a self-referencing pulstrode, Angew. Chem.-Int. Edit. 59 (2020) 2294-2298.